

COGENERATION AND DIESEL ELECTRIC POWER PRODUCTION

Final Report

by

Dr. Ronald A. Johnson
Institute of Northern Engineering
University of Alaska Fairbanks
Fairbanks, Alaska 99775-0660

September 1989

State of Alaska
Department of Transportation & Public Facilities
Research Section
Fairbanks, Alaska 99701

The contents of this report reflect the views of the author, who is responsible for the facts and the accuracy of the data presented herein. The contents do not necessarily reflect the official views or policies of the Alaska Department of Transportation and Public Facilities. This report does not constitute a standard, specification or regulation.

ABSTRACT

We have developed a data acquisition system to both monitor the efficiency of a diesel-electric generator set in producing electricity and to evaluate its performance as part of a cogeneration system for producing both heat and electricity. We have used this system to evaluate the performances of a 45 kW system consisting of a Mitsubishi engine coupled to a Stamford generator and an 80 kW Caterpillar system.

We find that, even though the efficiency of a generator set in producing electricity decreases appreciably as the electric load decreases, the cogeneration efficiency is relatively insensitive to load. The latter includes both the electric power produced and the rate of heat recovery from the jacket water as benefits. We also found that the engine temperature as measured by jacket water temperature can be maintained at high levels even at low loads if the cooling mechanism is restricted. We accomplished this in a laboratory situation by decreasing the water flow through an externally-mounted heat exchanger used to provide a source of cooling for the engine. We also found that the 80 kW cogeneration system at Coldfoot provided about one-third of the space heat needed by the maintenance shop. The payback period was less than 2 years for this system with about 2200 gallons of fuel oil being saved annually because of heat recovery from the jacket water.

Volume I contains the main body of the report; appendices are contained in Volume II.

ACKNOWLEDGEMENTS

I would like to acknowledge the help of John H. Martin and Mark Drygas from the DOT&PF maintenance section for helping us with our work at Coldfoot, Howard Furwirth and Charlotte Hok of the UAF INE for their invaluable assistance, and graduate students Mike Bethune, "Chilkoot" Ward, and Tay Epperson for helping to collect the data.

TABLE OF CONTENTS

	<u>Page</u>
ABSTRACT	ii
ACKNOWLEDGMENTS	iii
TABLE OF CONTENTS	iv
LIST OF FIGURES	v
LIST OF TABLES	vii
LIST OF APPENDICES	viii
INTRODUCTION	1
Background	1
Part Load Considerations	3
Waste Heat Recovery Considerations	7
PERFORMANCE OF 45 KW GENERATOR	12
Apparatus	12
Results	18
Discussion of Results	38
PERFORMANCE OF 80 KW GENERATOR	49
Apparatus	49
Results	51
Discussion of Results	52
ECONOMIC CONSIDERATIONS	59
CONCLUSIONS	62
REFERENCES	63
IMPLEMENTATION STATEMENT (by DOT&PF Statewide Research Section)	67
APPENDICES	Volume II

LIST OF FIGURES

	<u>Page</u>
Figure 1: Schematic of data logging system for 45 kW generator set	8
Figure 2: Test apparatus for 45 kW generator set	9
Figure 3: Schematic of 80 kW generator set instrumentation	13
Figure 4: 80 kW generator set	14
Figure 5: Temperature of jacket water leaving engine versus load for 45 kW generator set (numbers next to symbols represent shop water flow rates in gpm)	24
Figure 6: Oil temperature versus load for 45 kW generator set	25
Figure 7: Exhaust temperature versus load for 45 kW generator set	26
Figure 8: Heat rejected to jacket water versus load for 45 kW generator set	27
Figure 9: Heat rejected to shop water versus load for 45 kW generator set	29
Figure 10: Efficiency in producing electric power versus load for 45 kW generator set	30
Figure 11: Cogeneration efficiency versus load for 45 kW generator set	32

	<u>Page</u>
Figure 12: Cooling water temperatures versus time for 40 kW unmodified run using 45 kW generator set	33
Figure 13: Jacket water temperatures versus time for 40 kW unmodified run using 45 kW generator set	34
Figure 14: Water flow rates versus time for 40 kW unmodified run using 45 kW generator set	35
Figure 15: Exhaust temperature versus time for 40 kW unmodified run using 45 kW generator set	36
Figure 16: Fuel usage for 40 kW unmodified run using 45 kW generator set	37
Figure 17: Thermal and electrical outputs for 40 kW unmodified run versus time using 45 kW generator set	39
Figure 18: Energy balance for generator set	40
Figure 19: Heat delivered versus outdoor air temperature for 80 kW generator set	55

LIST OF TABLES

	<u>Page</u>
Table 1a: Basic thermodynamic and electrical steady state data for 45 kW generator set for initial runs	19
Table 1b: Basic thermodynamic and electrical steady state data for 45 kW generator set for final runs	20
Table 2a: Heat and efficiency results for 45 kW generator set for initial run	21
Table 2b: Heat and efficiency results for 45 kW generator set for final runs	22
Table 3: Coldfoot data. Average daily temperatures and flows	53
Table 4: Coldfoot data. Average daily heat flows and electric power	54

LIST OF APPENDICES (VOLUME II)

- A. Specifications for 4D31TM diesel
- B. Specifications for SC244C generator
- C. Specifications for Avtron load bank
- D. Specifications for OSI wattmeters
- E. Specifications for Lebow load cells
- F. Campbell 21X datalogger specifications
- G. Omega flowmeter specifications
- H. Program listing for 21X used for 45 kW generator tests
- I. Sample calculation for 10 kW normal run
- J. Specifications for 80 kW generator set
- K. Specifications for Bell and Gossett heat exchanger
- L. Specifications for Sponsler turbine flowmeters
- M. Program listing for 21X used for Coldfoot data acquisition
- N. Coldfoot raw data

INTRODUCTION

This final report is a discussion of the results obtained from two related research projects funded by DOT&PF. The first (Agreement 85NX086) involved a study of the economics and reliability of diesel electric generators and was conducted in two phases. The report for the first phase has already been written (Johnson et al., 1987). This report combines the second phase results from this study with those from a second research project (Agreement 87NX138) involving cogeneration. These two studies are closely linked as the former involved collecting performance and cogeneration data for a 45 kW system located at the School of Engineering at UAF while the latter involved the collection and analysis of field data on an 80 kW system. For each of these units, we are concerned with both the system performance in a cogeneration mode plus the effects of part loading on the amount of heat delivered.

Background

Diesel electric generators are widely used worldwide for the production of electric power in remote locations. Applications include electrification, agriculture, telecommunications, military/security, marine/navigation and cathodic protection. In this study we concentrated on electrification. Worldwide sales were 275 MW of installed capacity in 1983 with 45 MW of this in North America (Frost and Sullivan, 1985). As of 1979 in the U.S., there were 936 utility plants containing a total of 3,101 diesel engines for a total capacity of 5,117 MW. This represents 0.85% of the U.S. utility capacity

(Kirkwood, 1981). This same study reported that 86 of these plants, with total capacity of 291 MW, were located in Alaska and Hawaii. According to the 1986 Alaska Energy Plan (1986), the installed capacity in 1984 in Alaska was 277 MW which represented 17% of the total capacity.

Diesel engines became attractive in the U.S. in the 1920s because of the readily available inexpensive fuel oil and their higher efficiencies compared with steam engines and small steam turbines. An additional benefit was the greater operational flexibility compared with steam facilities. Other advantages are low initial costs, small space requirements, ease of transportability and a wide range of power capacities. Disadvantages include high maintenance costs, a relatively short operating life, high noise levels and the need for skilled labor to properly maintain the system.

In the U.S., 64% of the plants are under 1.5 MW in size with the average size being 1.6 MW. However, in Alaska and Hawaii, the average plant size is only 1.0 MW with 69% of the capacity in the base and intermediate service. Only one other region of the U.S., the South Atlantic, had over 50% of its capacity in fairly steady use. The average heat rate for plants in steady use is about 11,000 Btu/kWh which is 87% of that for the average fossil-fuel fired power station. The former translates into an efficiency of 31%. The cost of new diesel plants was about \$600/kW in the Lower 48, which was lower than new coal-fired plants. The annual U.S. market, according to Kirkwood (1981),

could be 400 MW/yr which is much larger than that estimated by Frost and Sullivan (1985).

The vast majority of Alaskan rural communities rely on diesel electric generators to supply their electric power needs. With the increase in government-funded housing, school construction, and community centers in many rural villages, the need for more energy has developed. In order to help offset the high cost of rural electricity generation, which is as high as \$0.55 per kWh in some villages, the Power Cost Equalization program was implemented to reduce the cost to the consumer (Keiser and Hoke, 1985). There is a lack of detailed and current information concerning energy use in rural Alaska, but we do know that in some villages only about 5% of the rural household energy use is for electricity, and over 50% is used for space heating. Hence, there is a real incentive to expand the use of cogeneration.

Part Load Considerations

The overall energy conversion efficiency of the generator set is one of the factors that determines the cost of producing electric power. The full-load efficiency of a diesel electric generator under ideal conditions is about 30%. If waste heat recovery is included the total efficiency can rise to over 60%. The part load electrical energy conversion efficiency of a diesel electric plant, however, is much less than the full-load value. Since stand-alone diesel electric plants are usually sized for peak demand, it is the part load performance of the system that easily can become the dominant influence on overall system efficiency. Furthermore, since most high-speed diesel engines cannot be

operated for long periods at much less than 40 to 60% load without eventually suffering from premature mechanical failures, the problem of how to deal with part load operation becomes a major concern of operators and system designers alike.

Reduced efficiency at part load is due in some measure to design deficiencies in the diesel engine because, in theory, the part load performance of the diesel is superior to that of any other reciprocating engine (Doolittle, 1964). Mechanical failures, of course, are related to other factors as well, such as improper maintenance, improper system specifications, and normal wear. In this section, however, we focus on part load problems of the diesel electric system to analyze the causes of the problem and consider what may be done to correct it.

The task of improving the part load efficiency of a diesel electric generator is twofold, but some solutions to one aspect of the problem also improve the other. The first part of the problem concerns the reduced efficiency of the diesel engine when it is operated at low loads. In most diesel engines, the thermal efficiency either remains constant or decreases as load decreases. The second aspect concerns modifications of the engine so that it can operate at less than 60% capacity without suffering mechanical failures. It is convenient that the modifications that will allow the diesel to operate at low loads will also increase the thermal efficiency.

Mechanical failures of diesel electric generators operated at low loads for long periods are primarily associated with poor combustion

processes. Good combustion requires that the ignition delay--the time between the start of injection and ignition--be as short as possible and that injected spray have a good distribution and mixing in the combustion chamber (Taylor, 1985). At part load both inlet air and combustion chamber temperatures fall, increasing ignition delay. Since most stationary diesels presently operate with fixed injection timing, increased ignition delay can cause combustion to occur well into the expansion stroke, which results in low output and poor efficiency (Campbell, 1979; Taylor, 1985). These factors, combined with low air and wall temperatures, promote the formation of carbon and varnish, which may build up on the valves, plug the injectors, and cause the piston rings to stick (Taylor, 1985).

An Alaska field survey (Malosh et al., 1986) reported on problems encountered by users relating to part loading. These included (a) hydrocarbon buildup, (b) rings sticking, (c) plugged injectors, (d) glazed pistons and cylinder walls, (e) "slobbering" (the emission of liquid hydrocarbons out the exhaust), (f) burning oil, and (g) shortened engine life. Of these problems, the one most often complained about was hydrocarbon buildup.

The field operators' recommendations for part load operation included: (a) using dummy loads (resistive load banks to absorb excess electrical output and keep engine loadings constant), (b) derating the fuel system, (c) periodically operating near full-load to purge hydrocarbon deposits, (d) keeping the block temperature high, (e) using an efficient fuel injection system, (f) sizing the generator set correctly, and (g)

instructing operators about the proper care and maintenance of diesel electric generator sets.

Much of the part load operation problem can be eliminated from the start by correctly sizing the generator to the immediate and near future (not long term) needs of the owner. If the engine is too large, it will have to run at a reduced load for an extended period and may ultimately fail before its expected design life. It will also cost more to run and maintain than if it were used more efficiently.

About two dozen manufacturers and vendors in the lower 48 states were contacted and, with two exceptions, said their systems should not be operated at part load for long periods of time. In response to a question about modifications to allow long-term operation at low loads without sustaining long-term mechanical problems, two vendors suggested an automatic radiator-mounted load bank. As the load on the generator falls below a preset level, a control circuit cuts in a load bank that is mounted on the radiator. The hot air from the load bank in turn heats the coolant and engine, thereby maintaining the coolant temperature. Automatic over-temperature controls are provided to keep the engine from overheating. This device is described in a reprint available from Avtron Manufacturing, Inc. ("Load Banks", n.d.). Besides the suggestion of load banks as solutions to part load problems, the most common reply was to use several properly sized units and run them in parallel for periods of maximum loads.

To provide more detailed data on generator set operational parameters at part loading, we performed several dozen tests at the University of Alaska Fairbanks using a 45 kW generator. To simulate the effects of dumping heat back into the engine at low loads to keep it warm, we restricted the shop water flow rate in the heat exchanger used to remove heat from the jacket water. This had the desired effect of maintaining high jacket water temperatures. We also performed tests with preheated intake air to help maintain engine temperatures at low loads. This only elevated the jacket water temperatures slightly. A schematic of the data logging system appears in Figure 1 and the equipment is pictured in Figure 2.

Waste Heat Recovery Considerations

The cogeneration of heat and electricity has become more common in the past decade. Roughly equal amounts of energy are found in electrical output, the jacket water and exhaust gas (each containing about 30% of the energy in input fuel) for a typical and properly operating diesel electric generator set. Hence, there exists the potential for substantial improvements in overall efficiency if some of this thermal energy can be recovered simultaneously with the generation of electricity.

There are a number of packaged cogeneration systems in the size range of 14 kW to 500 kW produced in the U.S. They include reciprocating engines and gas turbines (Mulloney, 1986). One widely used system is the TECOGEN module developed by Thermo Electron Co., of Waltham, MA. The 60 kW reciprocating spark ignition engine is fueled by natural gas, and

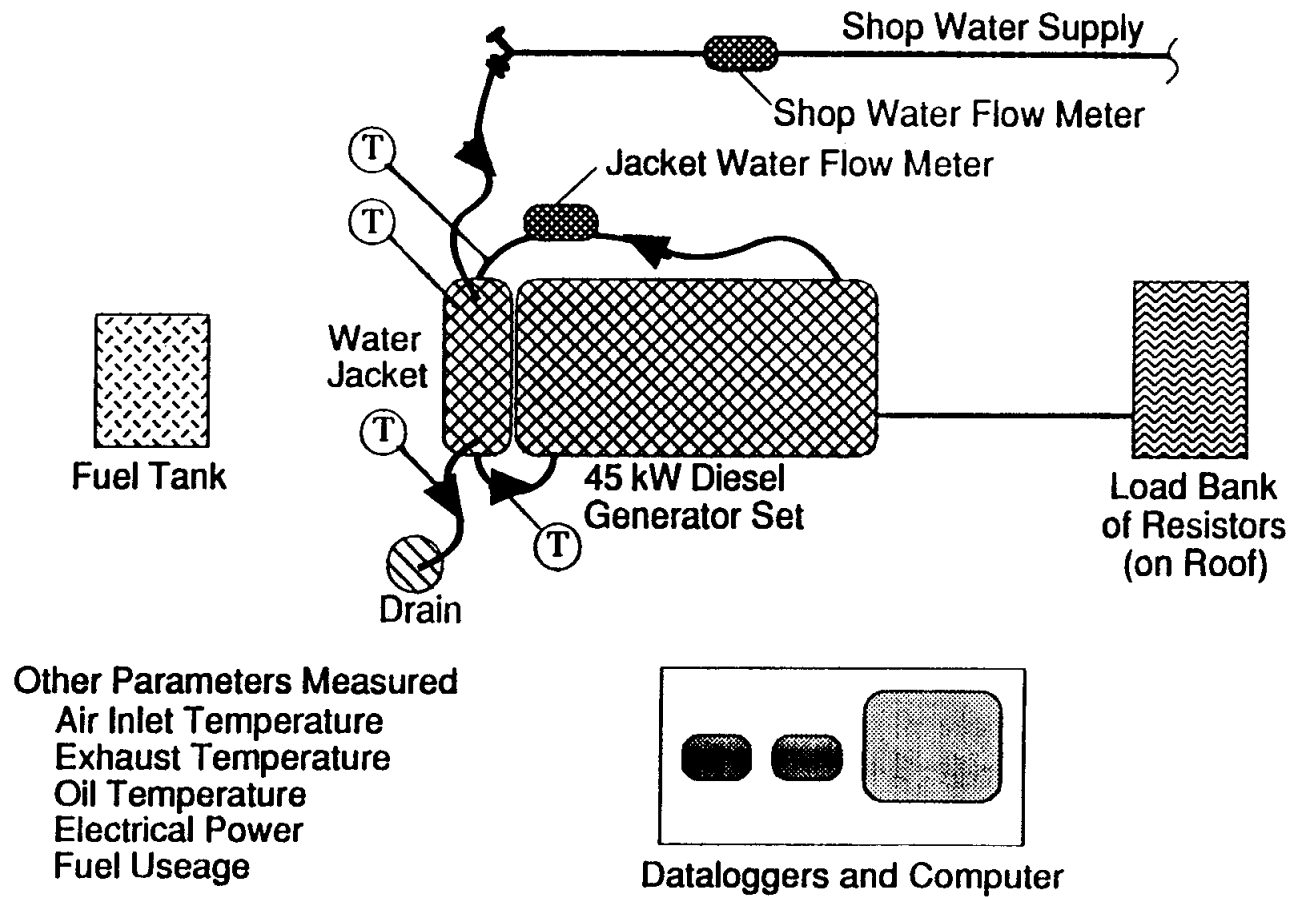


Figure 1. Schematic of data logging system for 45 kW generator set

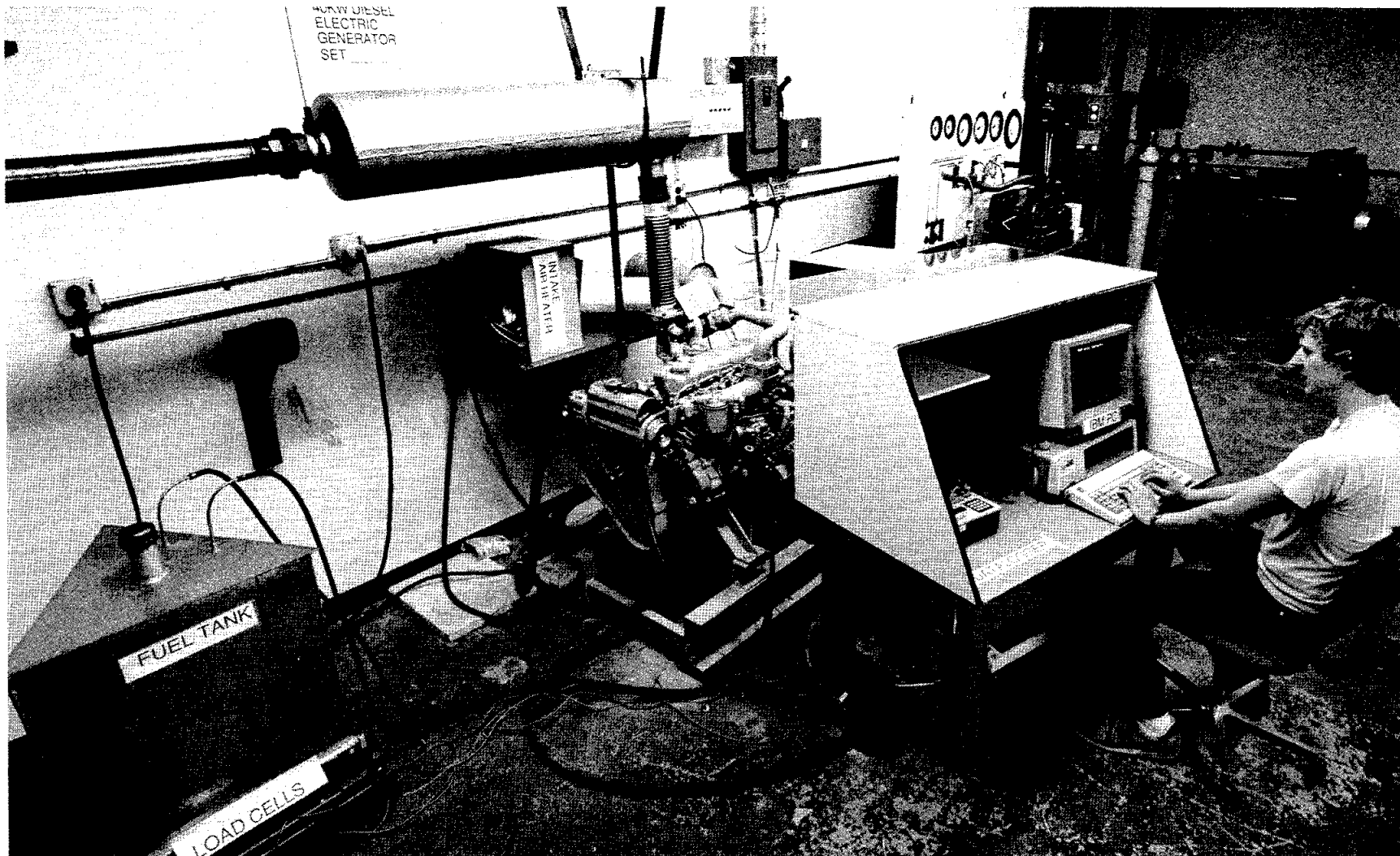


Figure 2. Test apparatus for 45 kW generator set

heat is recovered from both the jacket water and exhaust stack with a combined electrical and thermal efficiency of 85%. Experience with around 30 systems in the U.S. operating since as early as 1983 reveal an average capacity factor more than 67% and simple paybacks between 1.5 and 4 years. The installed cost is around \$1,300/kW (Sakhuja and Koplow, 1986).

In Alaska there are presently 12 minimally attended radar (MAR) sites which had or have diesel cogeneration systems with heat being recovered from either the jacket water or both jacket water and stack gas. Each energy system consists of four 175 kW or 250 kW diesel electric generators used in a cogeneration mode plus two 1.4 million Btu/hr diesel fueled boilers that can supply the entire thermal load in an emergency. The normal operating mode is two parallel generators equally sharing the load, one on hot standby, and one in reserve. Heat is recovered from the jacket water or stack gas by transferring to an ethylene glycol-water mixture at approximately 180°F. After passing through the shell and tube heat exchanger, the cooling water is either sent back to the engine directly or to remote radiators for further cooling. The overall cogeneration efficiency data were not available but the electrical efficiencies were over 34% except for one site at 29%. This site happened to have a Caterpillar rather than a Cummins diesel electric generator (Taylor et al., 1984).

At the present time, there are around a dozen operational heat recovery systems at Alaskan villages with two of these employing recovery of both stack gas and jacket water energy. The former has not been usually

practiced because of problems associated with stack corrosion when the stack gas is cooled below its dewpoint. The typical system consists of a shell and tube or plate heat exchanger to transfer heat from the jacket water to an external glycol-water loop that includes buried arctic pipe. This in turn transports the hot fluid to the end user which is usually a public facility such as a school. The entire system is custom designed for each individual site. The villages include Galena, Kaltag, Nome, Savoonga, St. Marys, Tanana, and Unalakleet. Similar systems have been used in at least four communities in the Northwest Territories in Canada (Cerigo and Ronton, 1984). The two oldest systems, installed in Unalaska and Ouzinkie, began operation in 1980. After monitoring for one year, simple payback periods of 2.5 and 9 years, respectively, were calculated (Hansen, 1987; Raj Bhargava Assoc., 1985).

Recently, 42 additional villages have been studied and 11 of these were recommended for heat recovery (Raj Bhargava Assoc., 1985). The estimated payback periods for these range from 5 to 10 years with projected annual savings from \$15 K to \$52 K. These savings consist mainly of fuel for heating and some in fan power for the radiator. Whether or not these are constructed depends upon the availability of state funds.

The recovered heat is used primarily for heating of boiler feedwater in public and large buildings. There have been numerous problems with the waste heat units according to Peter Hansen, project engineer for this construction program. These problems include leakage from seals, pipe

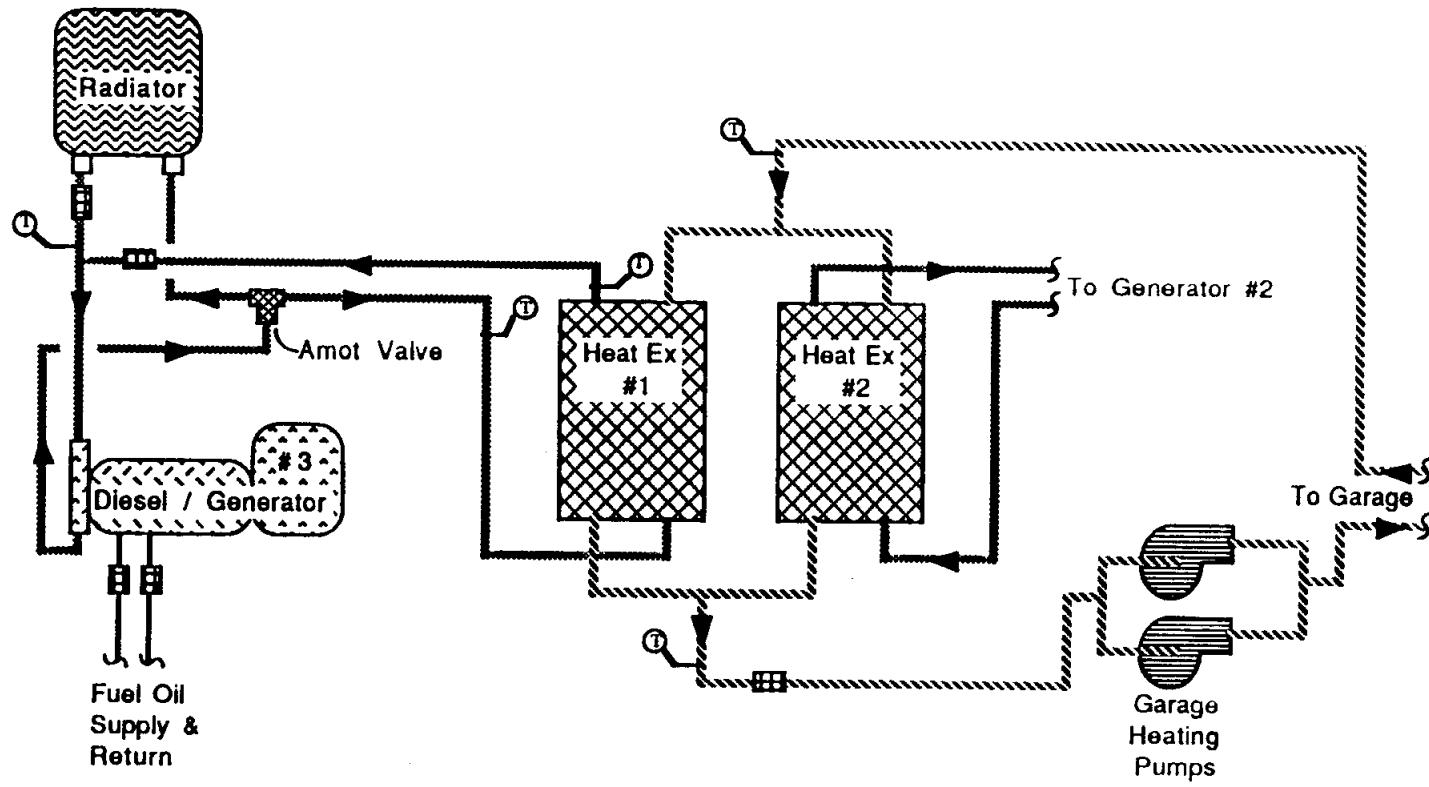
breakage, remote radiator fouling, defective British Thermal Unit meters and lack of village maintenance (Hansen, 1987). Most of the mechanical failures have been from underestimating the special operational and environmental concerns related to arctic and subarctic deployment of higher technology equipment. The anticipated fuel savings has not been realized, due to the maintenance problems and low loading of village generator sets. Because of these problems, the transferring of these systems from the Alaska Energy Authority to the local utilities had been delayed.

The field installation monitored in this project for its cogeneration performance was an 80 kW generator set at a DOT&PF maintenance camp in Coldfoot. For several months at the beginning of 1989, we monitored the heat being delivered to the shop building through a plate heat exchanger, as well as the electric power being delivered. Although waste heat was not recovered from the exhaust gas, we also measured exhaust gas temperature to help assess the potential for heat recovery from this stream. Figures 3 and 4 are a schematic of the critical components and a picture of the generator set respectively.

PERFORMANCE OF 45 KW GENERATOR

Apparatus

The specific apparatus used is a KEM MERLIN 45 kW generator set consisting of a Mitsubishi model 4D31TM diesel engine coupled to a Stamford model SC244C generator (Figure 2). The engine is a four cylinder, four stroke, in-line, watercooled, turbocharged unit running



Notes

- 1- Radiator coolant is ethylene glycol.
- 2- Hydronic fluid is propylene glycol.
- 3- All lines are 2" copper except the 1/2" copper fuel lines.

- ① Thermocouple well
 ☒ Turbine flow meter

Figure 3. Schematic of 80 kW generator set instrumentation

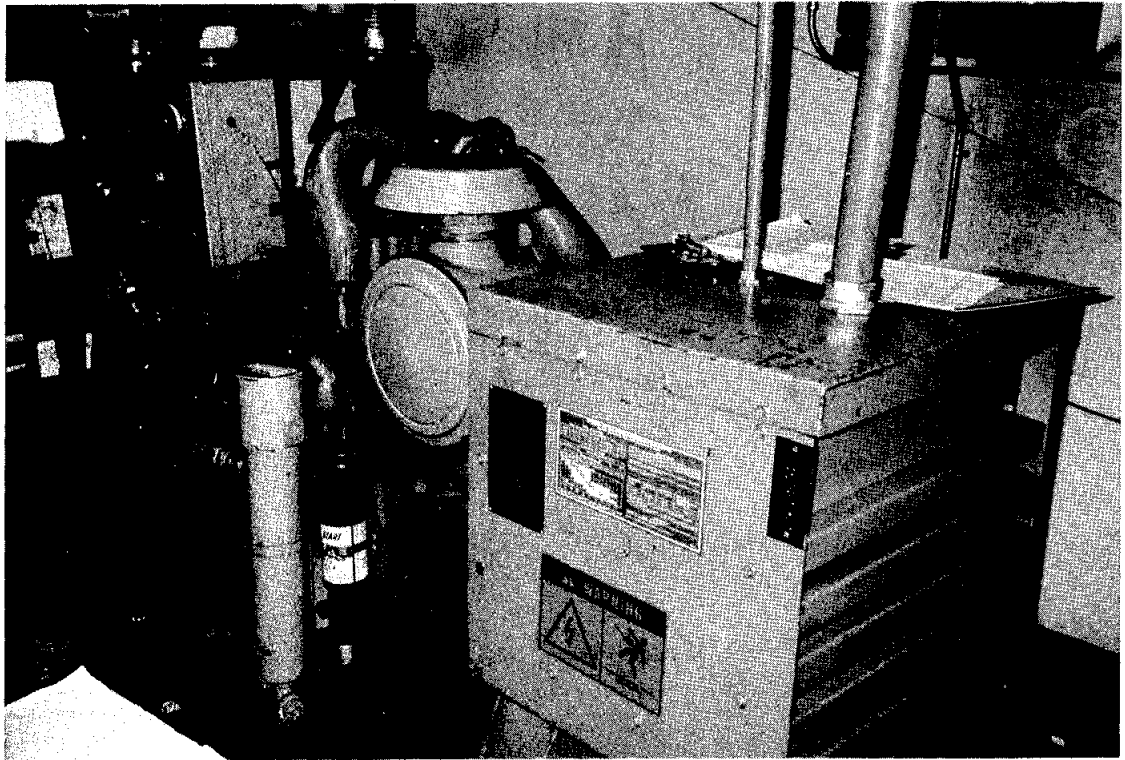


Figure 4. 80 kW generator set

at 1800 RPM. The generator is a directly connected A.C. revolving field type with 480 volts, three phase, four wire, and a power factor .80 or better. Jacket water heat is recovered using a unit mounted shell and tube heat exchanger. The electrical load is provided by an AVTRON Model K775 resistive load bank that can be stepped up in five kW increments. Details of these three items are provided in Appendices A, B, and C respectively.

The electric power output is sensed using an OSI wattmeter consisting of two current transformers and a voltmeter (Appendix D). The fuel consumption is monitored gravimetrically using Lebow load cells upon which the fuel tank rests (Appendix E). Critical system temperatures are measured using type T or K thermocouples and flow rates of water via Omega in-line turbine flowmeters. The output signals from these transducers (either in HZ or mV) are sent to a Campbell 21X datalogger (Appendix F) which is connected to a personal computer via an RS232 interface. Standard software plus some developed as part of this project is used to manipulate the data.

The weight of the fuel plus fuel tank at any instant of time is transmitted to three load cells. The resultant force creates an electrical signal by changing the electrical resistance of strain gages bonded to each cell. These gages are connected in a four arm Wheatstone bridge configuration. An output voltage proportional to applied load is developed after a fixed excitation voltage is applied using the data logger. From an independent calibration, the volume of number one diesel fuel in the tank is related to the load cell output by

$$V (\text{gal}) = 4.124 \text{ mV} - 10$$

Here, we have used a fuel density of 7.30 lbm/gal corresponding to number 1 diesel fuel. Because of background vibrations, there is a certain noise level associated with the load cell output. This is readily subtracted out by looking at the average slope of fuel remaining versus time over a time interval greater than 10 minutes.

When the coolant or other fluid passes through a turbine flowmeter an angular velocity is imparted to the rotor. This induces an AC voltage in a magnetic pickup coil mounted externally to the rotor. The frequency of this signal is proportional to the flowrate. For the Omega flowmeters used in these tests, 120 and 6,000 pulses per gallon were produced for the two inch and half inch flowmeters respectively (Appendix G). We programmed the 21X (Appendix H) to count the pulses over a five second interval. Hence, the number of pulses is multiplied by 0.1 to get the jacket water flow rate in gpm (two-inch flowmeter).

The Ohio Semitronics watt transducer produces a current proportional to the real power delivered to the load with a value of 1 mA at 80 kW. By placing a one k Ω resistor in the line, this becomes a one volt voltage which is easily stored in the 21X. Hence, the power in kW is the voltage times 80.

All the temperatures except for the exhaust gas were measured using precision grade type T thermocouples with limits of error of $\pm 0.9^\circ\text{F}$ or 0.4%, whichever is less. The exhaust gas temperature was measured using

type K precision grade thermocouple wire with limits of error of $\pm 1.8^{\circ}\text{F}$ or 0.4%. These resulted in signals of a few mV in magnitude being sent to the datalogger. They were then converted by polynomial curve fits into degrees F.

Independent parameters varied included the generator set loading (from about 13% to 93% in 5 or 10 kW increments), intake air temperature, and restricted versus unrestricted cooling. The first was accomplished by varying the number of electrical resistive elements activated on the load bank. To heat the intake air, an externally driven 9 kW electrical resistive heater was used. To vary the cooling, the flow rate of the shop water was decreased, which had the effect of increasing the jacket water temperature. A diagram of the data logger inputs is presented in Figure 1 and a photograph of the apparatus in Figure 2.

The purpose of performing the heated intake air and restricted cooling runs is to increase engine operating temperature at low loads. This should lessen the adverse effects associated with low temperatures discussed earlier. In a field operation, energy for heating intake air or jacket water could be obtained from heat released by a dummy load bank. Since our load bank was located four floors above the generator, it was easier for us to supply the heat externally to the intake air or increase jacket water temperature by restricting the shop water flow. By doing this, we are simulating feedback from a load bank in a field operation. In the latter (field) case, if the waste heat recovered is needed for space heating, we would not want to restrict the flow of the secondary circulating loop that supplies the space heating. Hence, we

would supply heat to the jacket water from a load bank during periods of low electrical demand.

Results

As mentioned already, the nominal test matrix consisted of runs extending from 5 kW up to essentially full load. In actuality, we performed tests at about 6, 11, 16, 21, 31, and 41 kW as evidenced in Tables 1a, 1b, 2a and 2b. These tables present the results for the steady state portions of the runs (representing averages over approximately five minutes) with some of the transient effects discussed later. Results for the critical temperature and flow data for each of the initial 15 runs performed are presented in Table 1a. It is apparent that the shop water temperature rises were much greater than the jacket water temperature drops through the heat exchanger because of the much greater flow rates of the latter. As expected, the exhaust temperature increased more or less uniformly with load over the entire range of loads, whereas the jacket water temperature coming out of the engine or into the heat exchanger was relatively constant with load for all the normal runs except one.

Similar data are found on Table 1b for a final set of runs. These were similar to the initial 15 runs except more temperature data were collected and the thermocouple wells were filled with a gel having a high thermal conductivity. For the first set of runs, the wells did not have a special substance inserted in them. The reasons for this modification are discussed later. Another difference is that the jacket

Table 1a: Basic thermodynamic and electrical steady state data for 45 kW generator set for initial runs

Normal Run									
Power elec.	Flow sw	Flow jw	Tsi	Tso	Tji	Tjo	Toil	Tex	Tair
[kW]	[gpm]	[gpm]	[°F]	[°F]	[°F]	[°F]	[°F]	[°F]	[°F]
5.80	1.20	0.00	64.80	130.20	140.30	171.00	163.50	385.70	-
11.00	2.50	21.50	65.20	99.30	169.50	175.30	162.10	461.00	-
16.20	2.80	22.80	62.40	105.10	168.60	175.20	-	532.60	76.70
21.30	3.70	17.60	63.70	96.80	165.30	174.80	164.50	627.10	-
31.30	4.30	28.80	64.40	97.50	168.90	176.40	168.20	776.30	-
41.40	4.30	34.00	66.00	106.20	183.00	191.00	186.10	926.40	-
Restricted Run									
Power elec.	Flow sw	Flow jw	Tsi	Tso	Tji	Tjo	Toil	Tex	Tair
[kW]	[gpm]	[gpm]	[°F]	[°F]	[°F]	[°F]	[°F]	[°F]	[°F]
5.80	1.10	26.30	65.70	145.90	198.40	202.80	-	391.50	85.30
10.90	1.30	26.20	65.20	147.10	201.60	206.60	-	466.10	86.70
16.00	1.50	25.90	65.80	133.70	181.20	186.90	-	543.70	88.90
21.30	2.20	25.80	66.50	122.60	198.60	205.20	-	642.00	92.40
31.50	3.20	25.70	66.50	116.90	186.30	194.40	-	790.90	92.50
Heated Run									
Power elec.	Flow sw	Flow jw	Tsi	Tso	Tji	Tjo	Toil	Tex	Tair
[kW]	[gpm]	[gpm]	[°F]	[°F]	[°F]	[°F]	[°F]	[°F]	[°F]
5.80	1.80	35.60	71.00	117.80	181.90	185.50	144.40	416.40	-
11.00	1.50	6.70	70.80	136.80	156.00	173.80	140.40	491.40	-
16.10	2.90	33.60	69.20	107.70	171.50	176.60	138.50	577.00	-
21.30	3.20	33.90	69.60	107.70	172.50	178.30	139.70	673.10	-

Notes for Tables 1a,b and 2a,b:

The shop water (sw) refers to the building water used on the cool side of the heat exchanger to remove heat from the jacket water (jw) on the hot side. The designators "si", "so", "ji", and "jo" (flows in and out) refer to the heat exchanger for the shop water and to the engine for the jacket water, while "ex" refers to the exhaust. "T" indicates temperature and "Flow" indicates volume flow rate. The latter is expressed in gpm. Heat Flow "h" is the energy input rate via the fuel.

Table 1b: Basic thermodynamic and electrical steady state data for 45 kW generator set for final runs

Normal Run

Power elec. [kW]	Flow sw [gpm]	Flow jw [gpm]	Tsi [°F]	Tso [°F]	Tji [°F]	Tjo [°F]	Toil [°F]	Tex [°F]	Tair [°F]
5.78	2.04	9.66	68.10	107.70	164.37	174.31	174.01	400.55	94.36
10.82	2.07	32.89	67.97	116.26	173.86	177.52	179.72	471.45	90.60
10.86	3.90	4.65	67.99	94.98	144.11	172.39	174.80	468.85	89.90
11.08	1.98	33.71	68.80	116.48	178.10	181.63	182.36	483.02	96.66
21.51	4.11	10.54	68.54	101.65	157.92	172.72	180.09	657.20	99.08
31.89	4.07	32.09	69.53	116.19	170.63	177.10	189.24	828.60	103.08
41.69	4.11	32.80	69.03	123.11	178.07	185.62	197.90	978.45	100.90

Restricted Run

Power elec. [kW]	Flow sw [gpm]	Flow jw [gpm]	Tsi [°F]	Tso [°F]	Tji [°F]	Tjo [°F]	Toil [°F]	Tex [°F]	Tair [°F]
10.79	2.46	25.70	67.19	111.40	165.59	170.83	174.56	471.77	-
10.79	1.22	25.74	67.58	160.65	206.22	210.48	198.23	481.58	-
10.87	4.12	25.71	67.75	94.69	139.40	145.26	156.55	460.97	-
21.54	2.12	25.23	68.84	132.03	188.78	195.56	199.39	663.08	-
21.51	4.10	25.38	68.20	103.03	153.26	160.64	172.10	644.20	-
31.80	3.06	25.05	68.08	124.79	178.83	187.51	199.70	823.03	-
31.78	3.09	24.23	68.40	126.40	182.26	191.02	193.40	829.12	-

Table 2a: Heat and efficiency results for 45 kW generator set for initial run

Normal Run							
Power elec. [kW]	Flow sw [gpm]	Flow jw [gpm]	Heat Flow h [kW]	Heat Flow sw [kW]	Heat Flow jw [kW]	Elec. Eff. [%]	Cogen. Eff. [%]
5.80	1.20	0.00	37.60	11.60	0.00	15.43%	46.28%
11.00	2.50	21.50	48.90	12.30	18.40	22.49%	47.65%
16.20	2.80	22.80	59.80	17.70	22.10	27.09%	56.69%
21.30	3.70	17.60	73.00	18.10	24.30	29.18%	53.97%
31.30	4.30	28.80	101.00	21.10	31.60	30.99%	51.88%
41.40	4.30	34.00	128.10	25.20	40.20	32.32%	51.99%
Restricted Run							
Power elec. [kW]	Flow sw [gpm]	Flow jw [gpm]	Heat Flow h [kW]	Heat Flow sw [kW]	Heat Flow jw [kW]	Elec. Eff. [%]	Cogen. Eff. [%]
5.80	1.10	26.30	37.60	12.60	16.80	15.43%	48.94%
10.90	1.30	26.20	48.40	15.30	19.10	22.52%	54.13%
16.00	1.50	25.90	60.30	15.20	21.70	26.53%	51.74%
21.30	2.20	25.80	73.00	18.20	24.90	29.18%	54.11%
31.50	3.20	25.70	98.20	23.60	30.40	32.08%	56.11%
Heated Run							
Power elec. [kW]	Flow sw [gpm]	Flow jw [gpm]	Heat Flow h [kW]	Heat Flow sw [kW]	Heat Flow jw [kW]	Elec. Eff. [%]	Cogen. Eff. [%]
5.80	1.80	35.60	35.20	12.30	18.60	16.48%	51.42%
11.00	1.50	6.70	49.90	14.20	17.50	22.04%	50.50%
16.10	2.90	33.60	61.50	16.30	25.40	26.18%	52.68%
21.30	3.20	33.90	77.20	18.20	28.70	27.59%	51.17%

Table 2b: Heat and efficiency results for 45 kW generator set for final runs

Normal Run								
Power elec.	Flow sw	Flow jw	Heat Flow h	Heat Flow sw	Heat Flow jw	Elec. Eff.	Cogen. Eff.	Fuel Flow
[kW]	[gpm]	[gpm]	[kW]	[kW]	[kW]	[%]	[%]	[gpm]
5.78	2.04	9.66	35.54	11.78	11.97	16.27%	49.41%	0.0144
10.82	2.07	32.89	45.47	14.57	15.54	23.81%	55.85%	0.0185
10.86	3.90	4.65	47.46	15.37	16.95	22.89%	55.28%	0.0193
11.08	1.98	33.71	42.64	13.79	15.35	25.99%	58.32%	0.0173
21.51	4.11	10.54	72.90	19.88	20.12	29.50%	56.77%	0.0296
31.89	4.07	32.09	104.36	27.72	26.77	30.56%	57.12%	0.0424
41.69	4.11	32.80	129.66	32.44	31.96	32.15%	57.17%	0.0526
Restricted Run								
Power elec.	Flow sw	Flow jw	Heat Flow h	Heat Flow sw	Heat Flow jw	Elec. Eff.	Cogen. Eff.	
[kW]	[gpm]	[gpm]	[kW]	[kW]	[kW]	[%]	[%]	
10.79	2.46	25.70	46.96	15.89	17.35	22.98%	56.81%	
10.79	1.22	25.74	46.20	16.58	14.13	23.35%	59.24%	
10.87	4.12	25.71	49.47	16.22	19.41	21.97%	54.76%	
21.54	2.12	25.23	72.03	19.55	22.07	29.90%	57.05%	
21.51	4.10	25.38	72.50	20.87	24.16	29.67%	58.46%	
31.80	3.06	25.05	98.90	25.38	28.04	32.15%	57.82%	
31.78	3.09	24.23	98.53	26.18	27.37	32.25%	58.82%	

fluid was distilled water for the initial runs and a 50% ethylene glycol-50% water mixture for the final set of runs.

Some of the critical temperature data are plotted in Figures 5-7 with the jacket water temperature leaving the engine appearing on Figure 5. By comparing average values across the different loadings, it is apparent that the jacket water temperature only changed appreciably for the highest power level, 40 kW, for the normal runs and was slightly elevated at the lowest load for the heated intake air run. The most noticeable effect occurred for the restricted cooling runs where the jacket water temperatures were significantly effected by the shop water flow rates. The shop water flow rates are indicated on Tables 1a and 1b. The oil temperature (Figure 6, Tables 1a and 1b) was elevated also for the restricted cooling runs at low shop water flow rates and increased somewhat with load at the highest power level tested for the normal runs. The exhaust temperature (Figure 7) increased by over 500°F from the lowest to the highest power levels.

The heat rejected to the jacket water as a function of load appears in Figure 8. Its magnitude is of the order of the electric power produced. The rate of heat input into or out of a heat exchanger is calculated from an energy balance

$$\dot{Q} = \dot{m} c_p (T_i - T_e) \quad (1)$$

where \dot{m} is the mass flux of fluid, c_p its specific heat, T is temperature, and the subscripts i and e denote conditions into and out of the heat exchanger respectively.

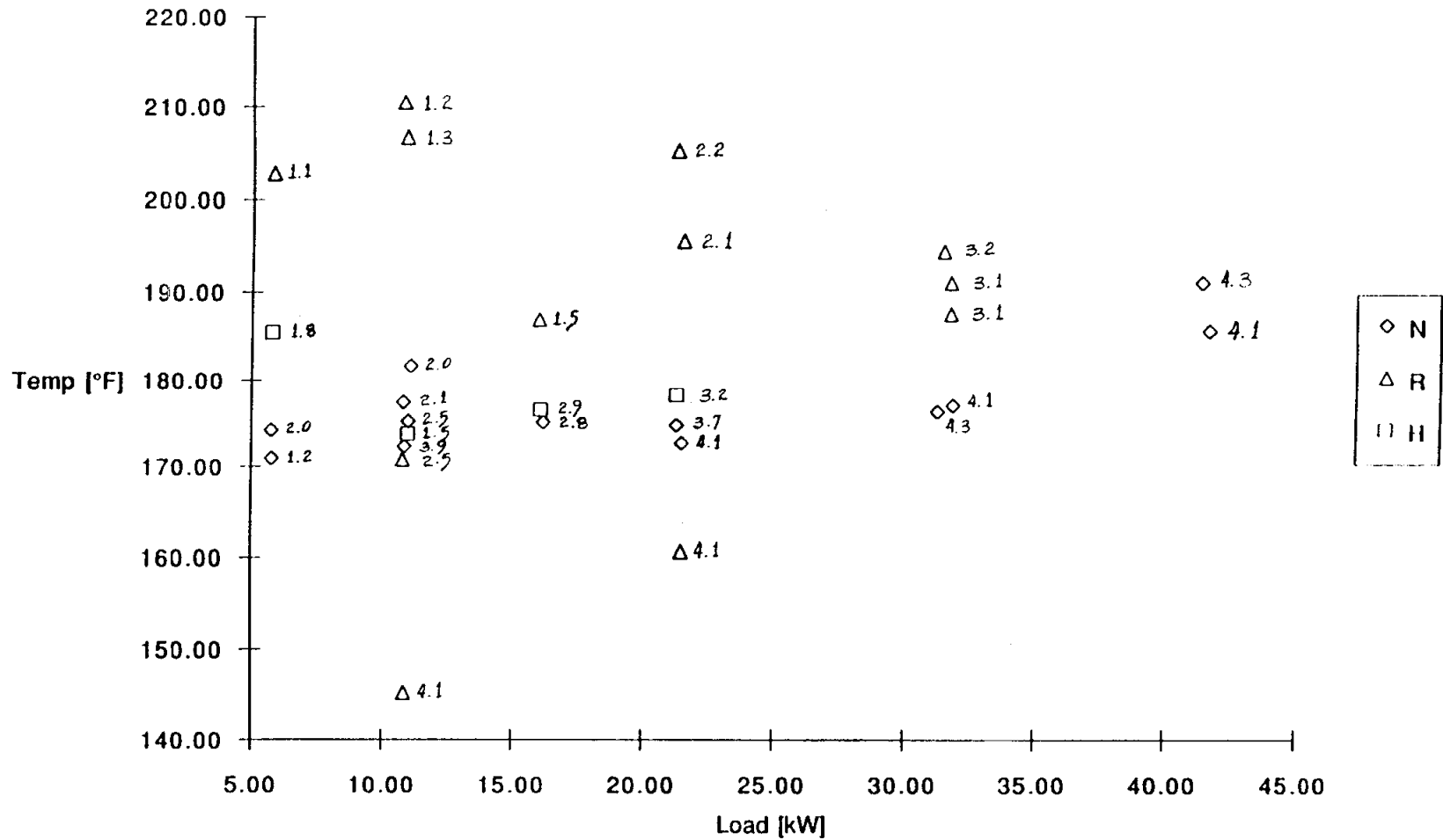
T_{jo} vs Load

Figure 5. Temperature of jacket water leaving engine versus load for 45 kW generator set (numbers next to symbols represent shop water flow rates in gpm)

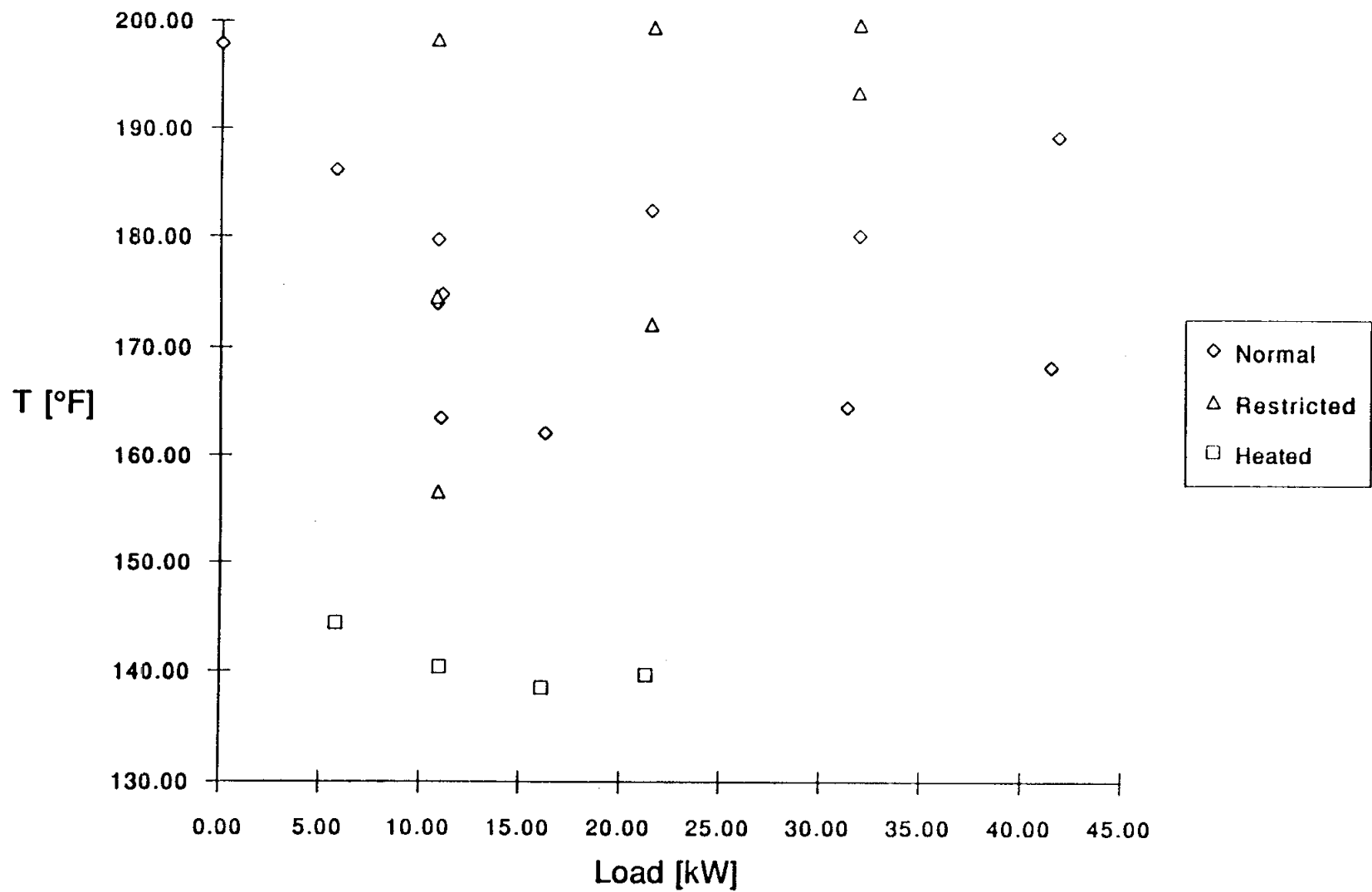


Figure 6. Oil temperature versus load for 45 kW generator set

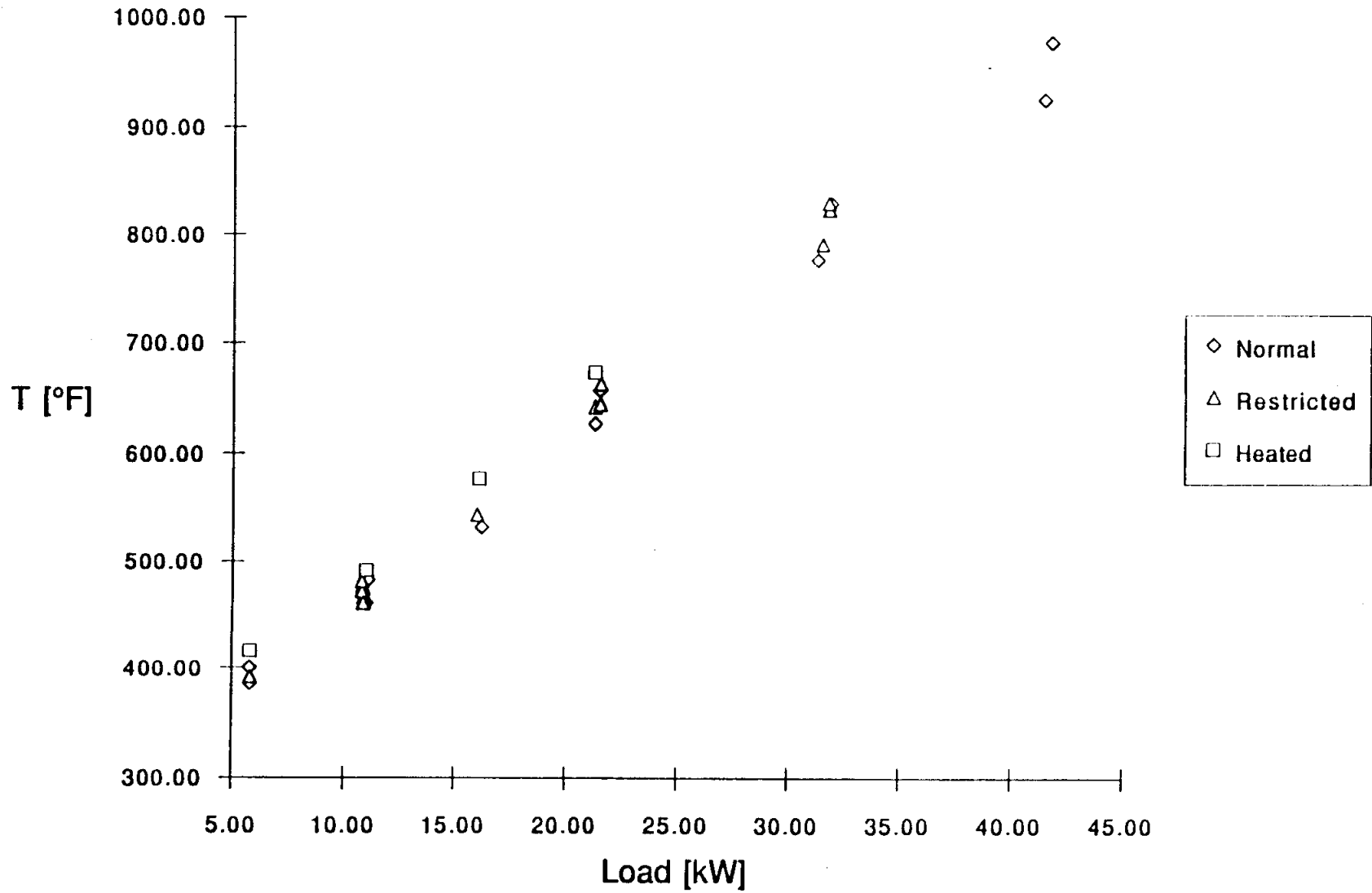


Figure 7. Exhaust temperature versus load for 45 kW generator set

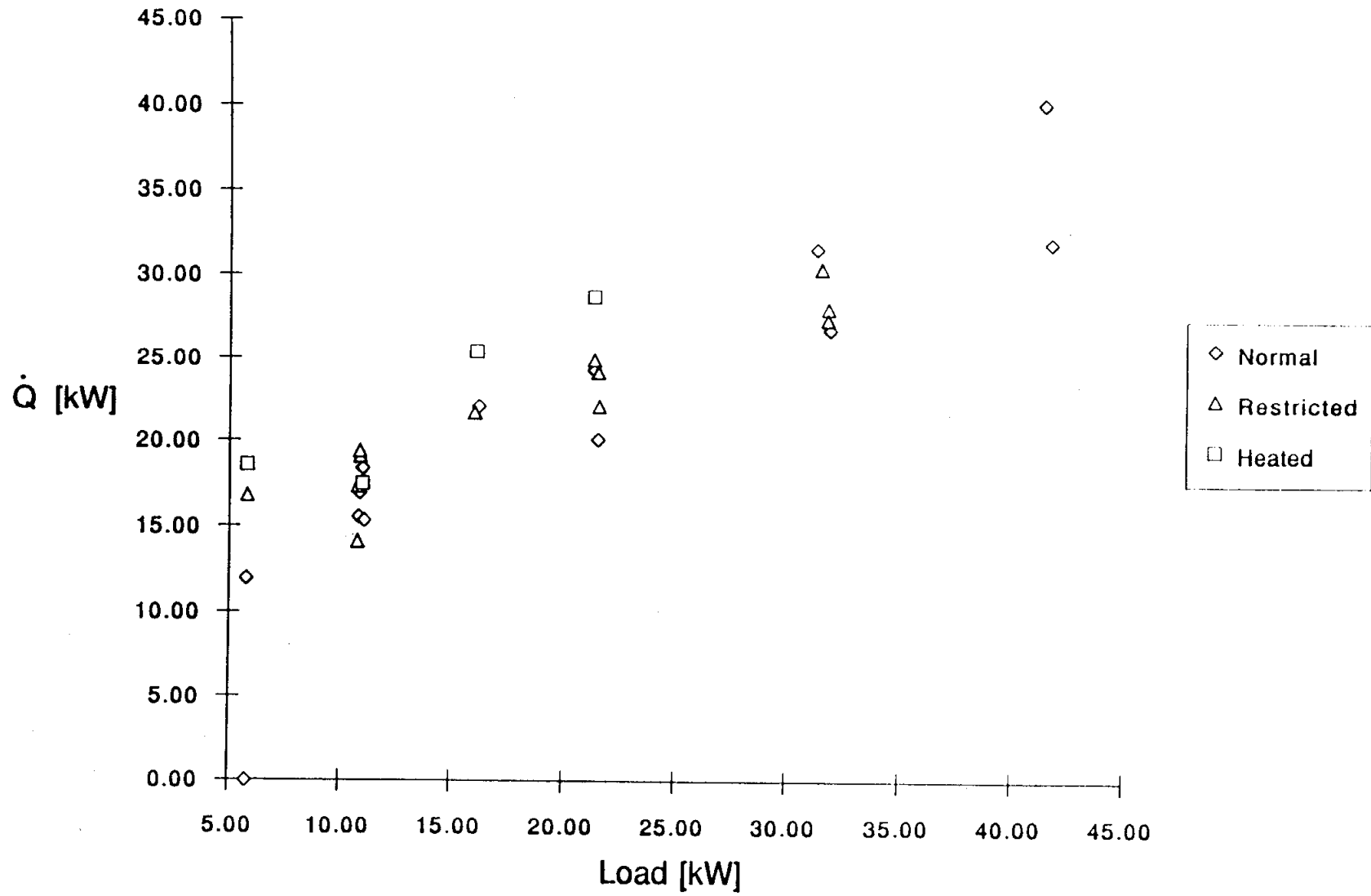


Figure 8. Heat rejected to jacket water versus load for 45 kW generator set

The heat rejected at a given load is generally elevated by 10-20% by heating the intake air just as the exhaust gas temperature is higher in the heated air runs.

The corresponding plot for shop water appears on Figure 9. Here, there is less variation in rejected heat at a given load for the lower power levels. Part of this is related to our ability to measure shop water temperature rise more accurately than jacket water temperature drop for the initial runs. The efficiency in producing electric power (Figure 10) increases with load with differences between the normal and restricted runs at a given load being generally small. Here, we have defined electrical efficiency by

$$\eta_{el} = \dot{W}_{el} / \dot{Q}_h \quad (2)$$

where \dot{W}_{el} is the electrical power output of the generator and \dot{Q}_h is the energy input rate in the fuel. We have used number one diesel fuel and used the higher heating value of 140,400 Btu/gal (Taylor, 1985). For the heated air runs, the efficiency defined this way is slightly higher at the lowest load because we haven't accounted for the energy input by the air heater. If we do, each electrical efficiency falls by about 3%, making the heated air efficiencies lower than the other two at all loads.

We have defined cogeneration efficiency in Figure 11 as

$$\eta_{cog} = (\dot{W}_{el} + \dot{Q}_{sw}) / \dot{Q}_h \quad (3)$$

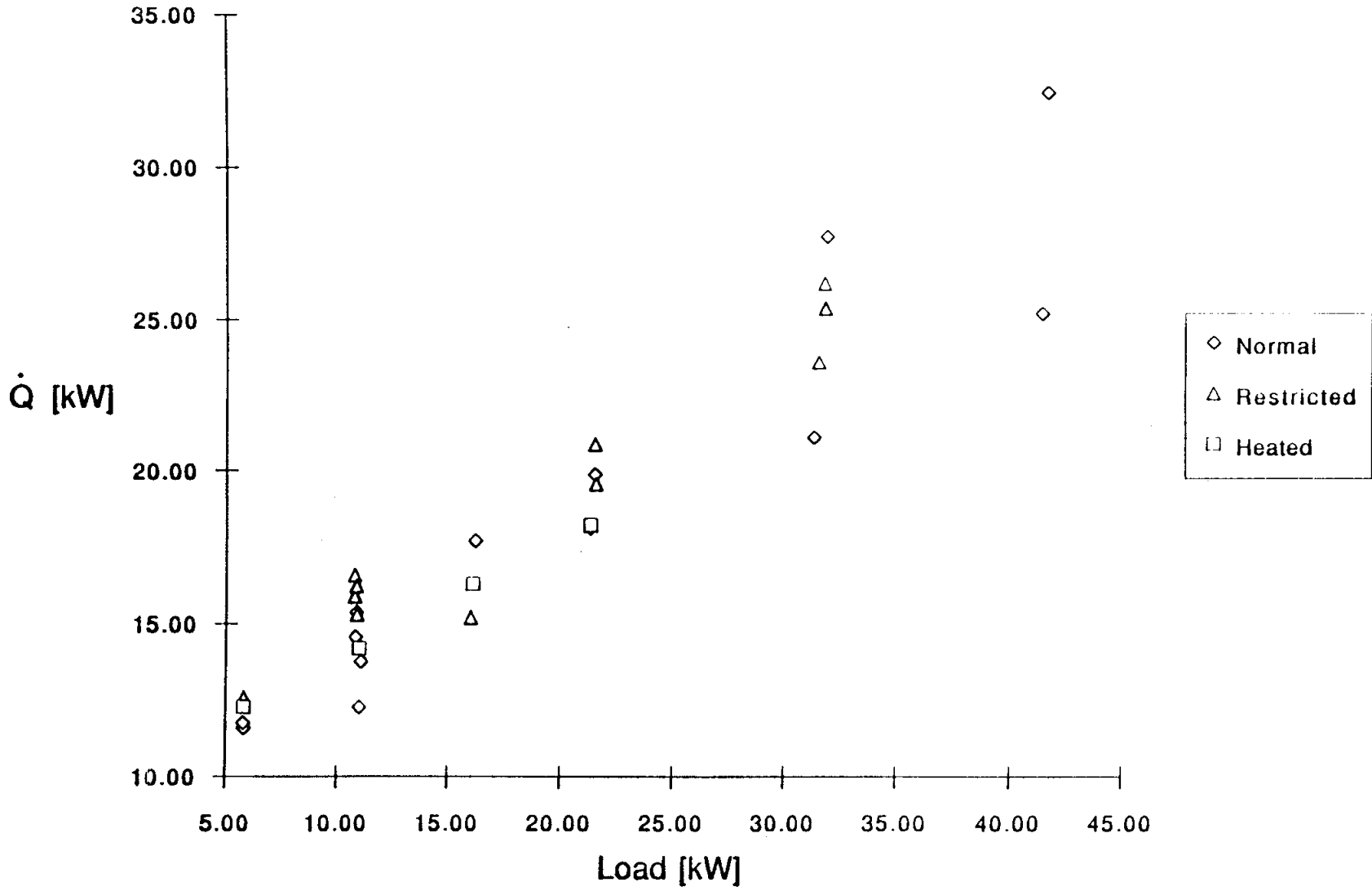


Figure 9. Heat rejected to shop water versus load for 45 kW generator set

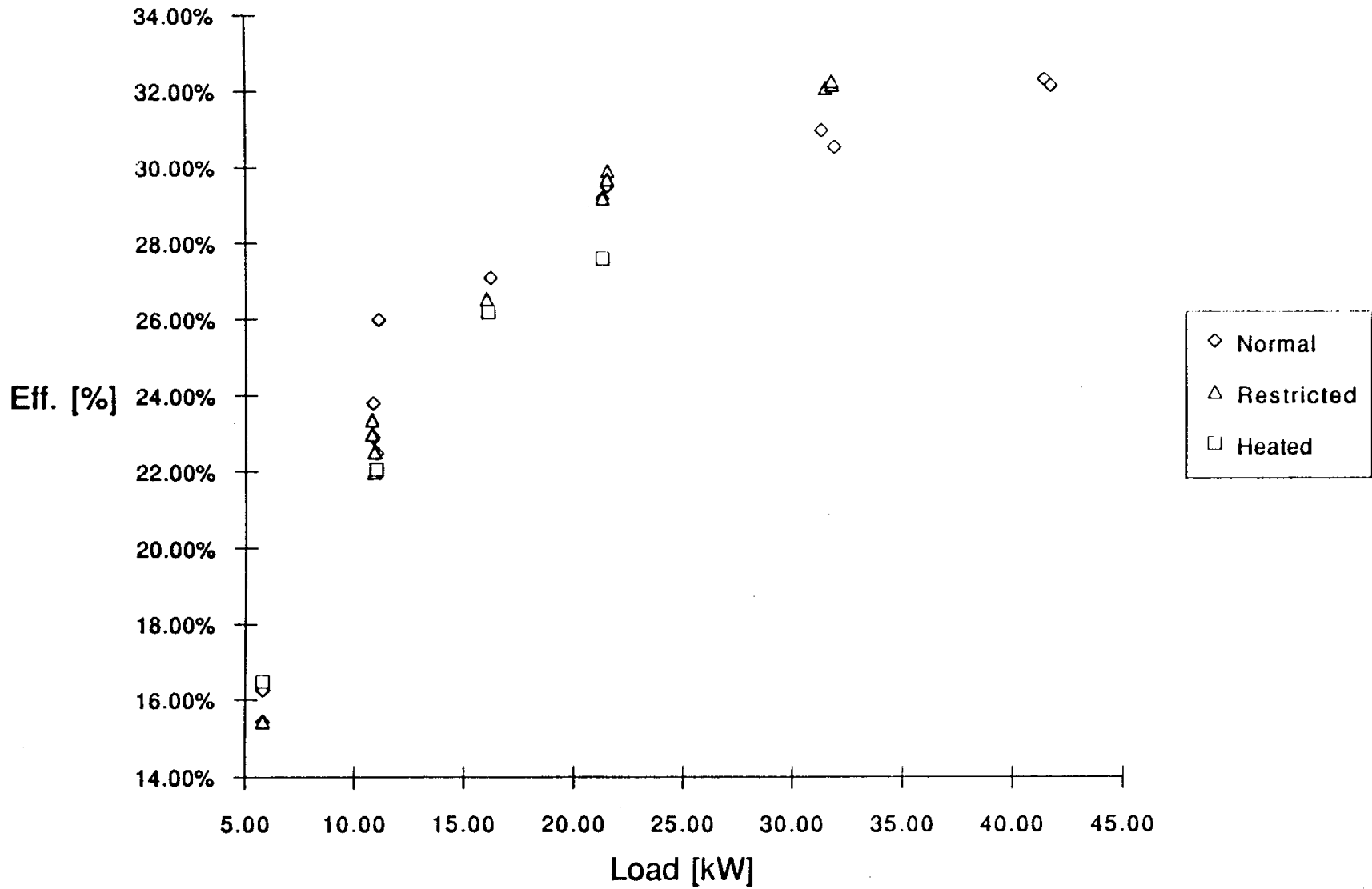


Figure 10. Efficiency in producing electric power versus load for 45 kW generator set

where \dot{Q}_{sw} is the heat rejection rate to the shop water. It is essentially invariant with load for the normal and restricted runs except for the lowest loads. The variation with load is due to different shop water flow rates. For the heated air runs, the efficiencies defined by Equation 3 appear to be higher than for some of the other runs. This is because we don't account for the energy input by the air heater using the above equation. If this input is taken into account, then the heated intake cogeneration efficiencies are always lower than for the other two cases, similar to the electrical efficiency results.

It should be noted that the nominal 10 kW heated air results on Table 2a do not represent steady state conditions, as the jacket water flow rate was still increasing near the termination of the run (2400 secs). To provide some information on the transient portions of our test matrix, we have shown plots of significant independent variables versus time for the nominal 40 kW unmodified or normal initial run on Figures 12 through 17. The cooling or shop water outlet temperature increased with time (Figure 12) as the engine jacket water temperature increased (Figure 13). The jacket water temperatures (Figure 13) fluctuated slightly during 5 minutes of the run as the thermostat opened and closed. The jacket water flow rate (Figure 14) reached a steady state value after about 10 minutes, while the shop water flow rate varied slightly due to other demands in the building. The exhaust temperature approached steady state after about 30 minutes (Figure 15). The best fit curve for the fuel usage in time (Figure 16) led to a calculated fuel consumption rate of 0.0519 gpm. The fluctuations in these data are due to

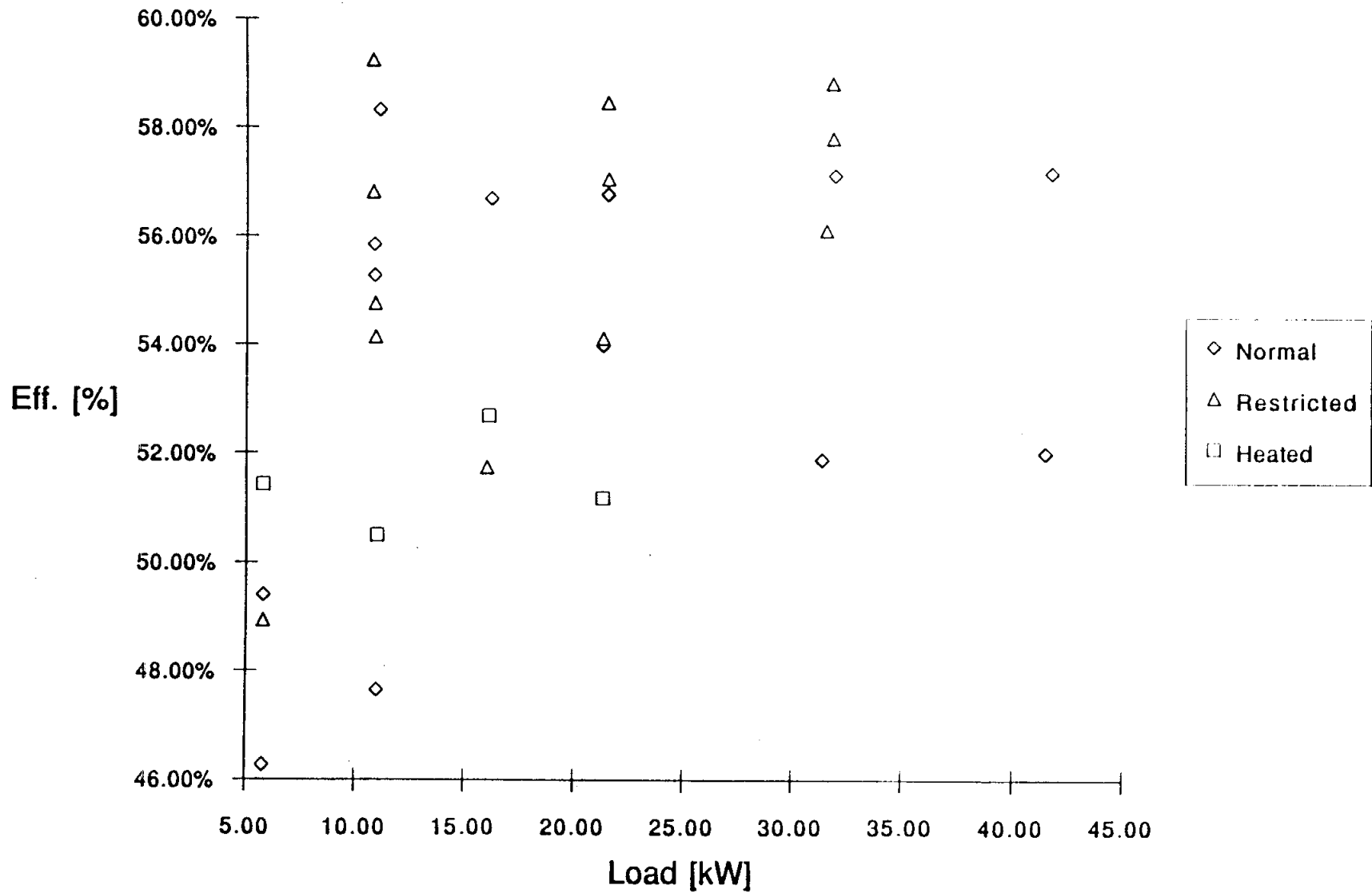


Figure 11. Cogeneration efficiency versus load for 45 kW generator set

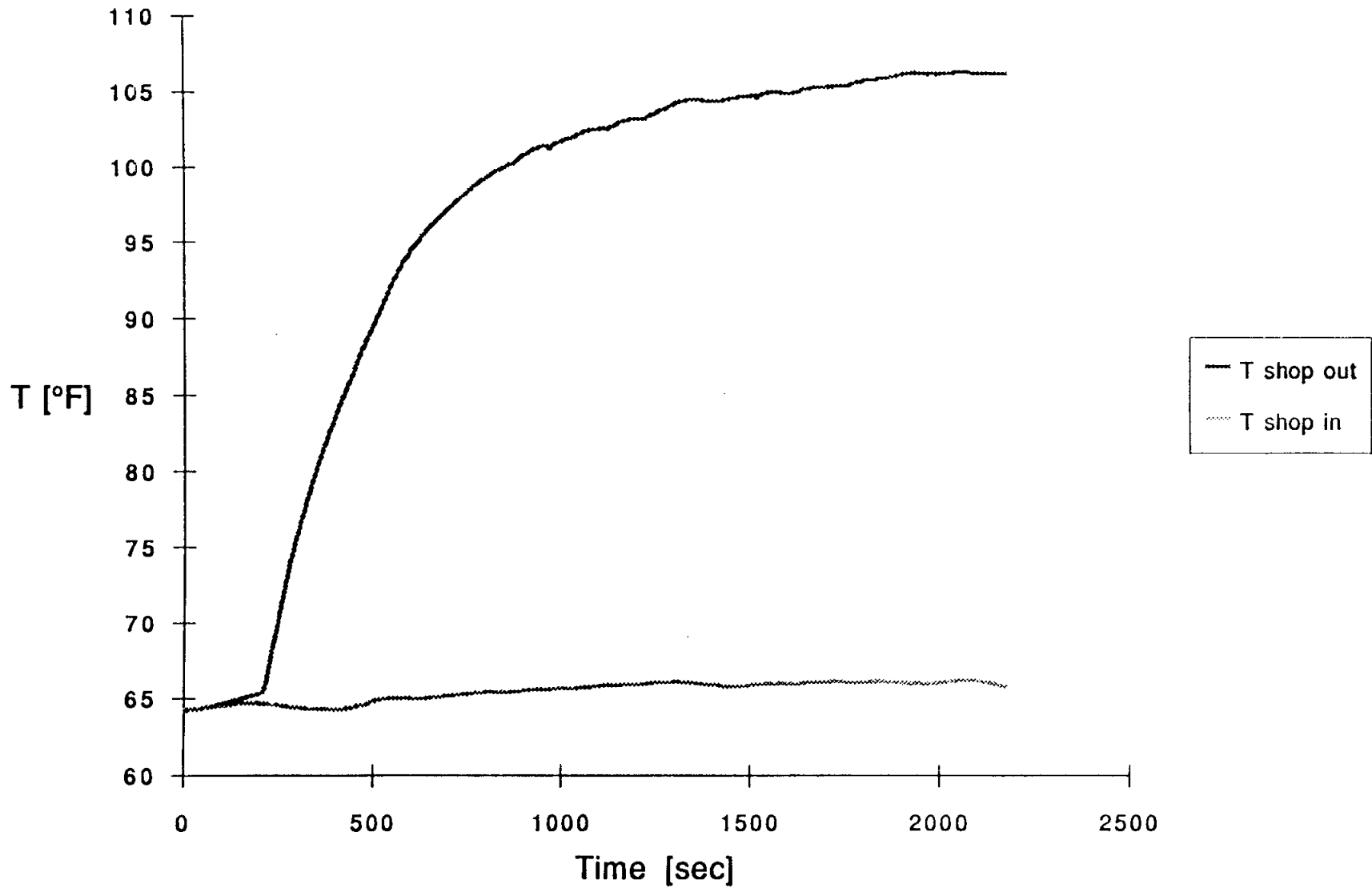


Figure 12. Cooling water temperatures versus time for 40 kW unmodified run using 45 kW generator set

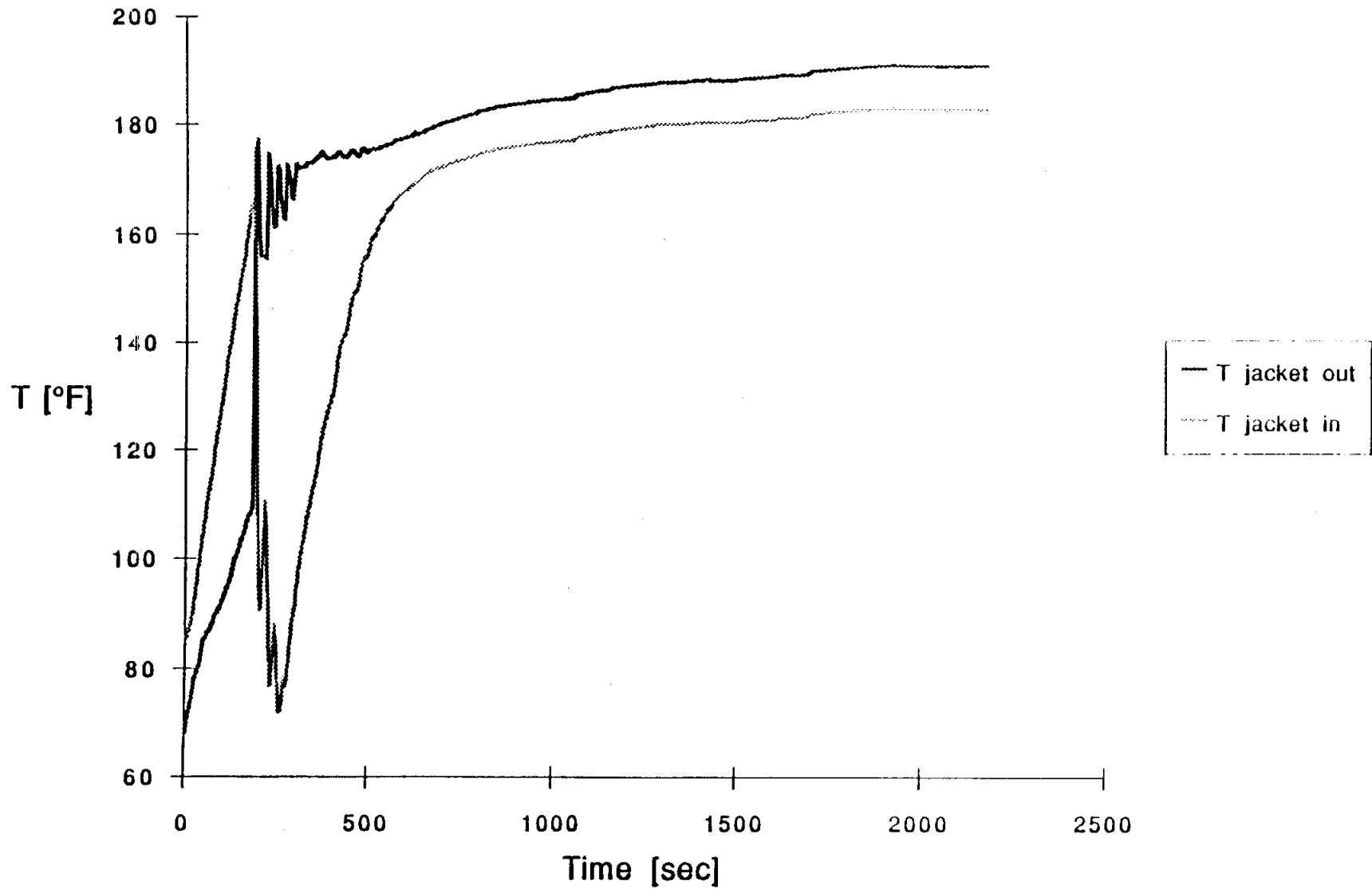


Figure 13. Jacket water temperatures versus time for 40 kW unmodified run using 45 kW generator set

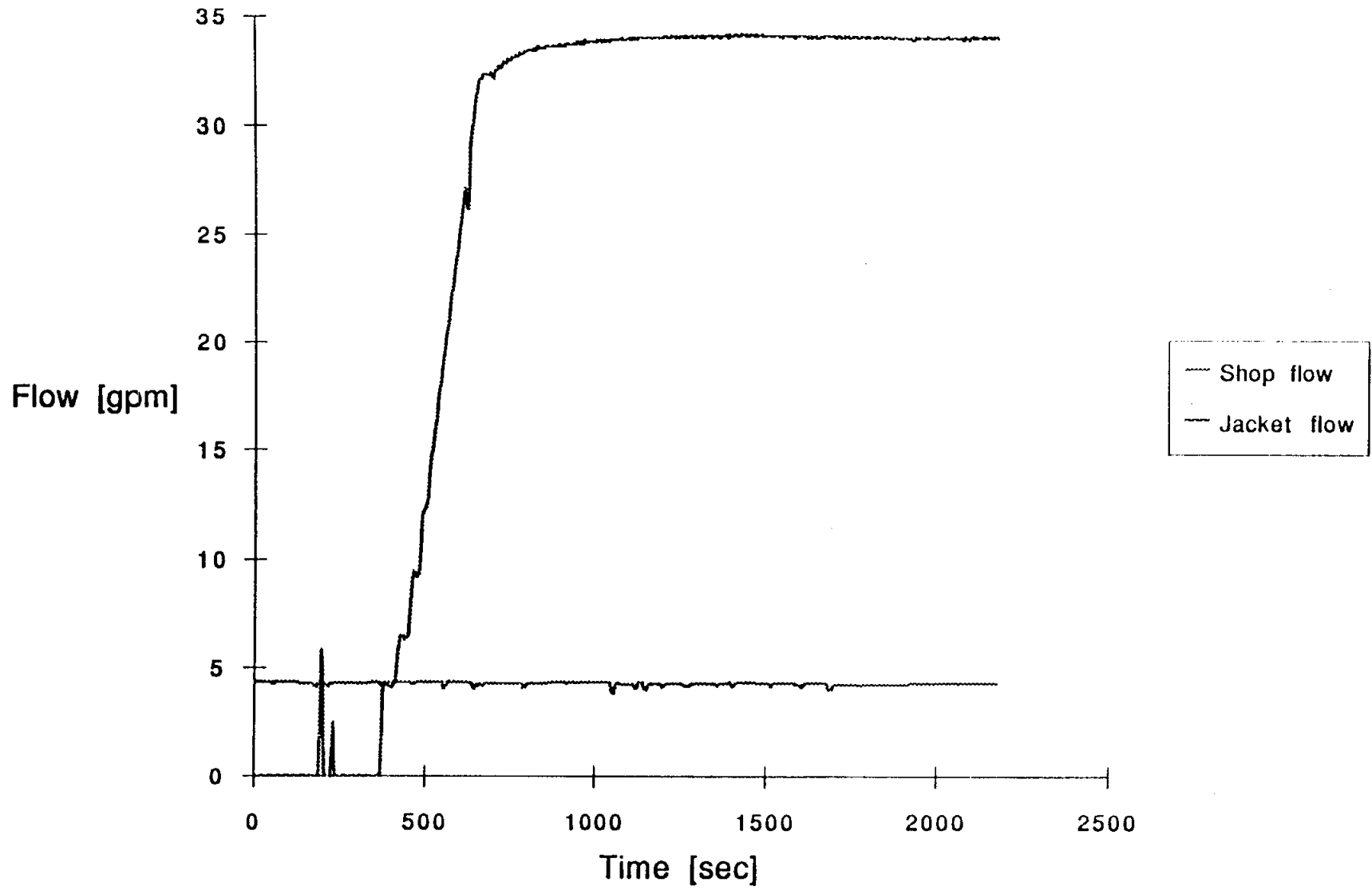


Figure 14. Water flow rates versus time for 40 kW unmodified run using 45 kW generator set

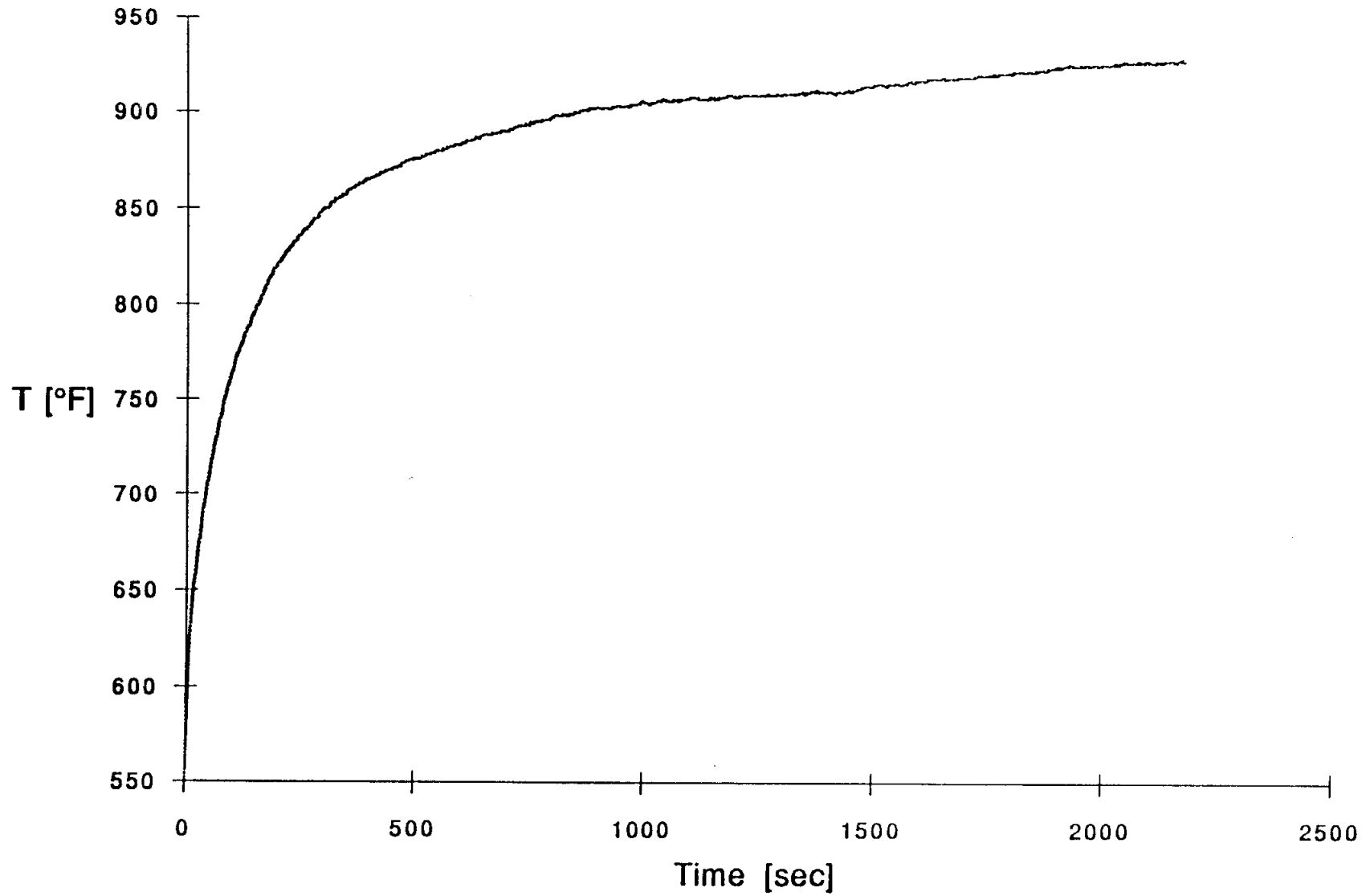


Figure 15. Exhaust temperature versus time for 40 kW unmodified run using 45 kW generator set

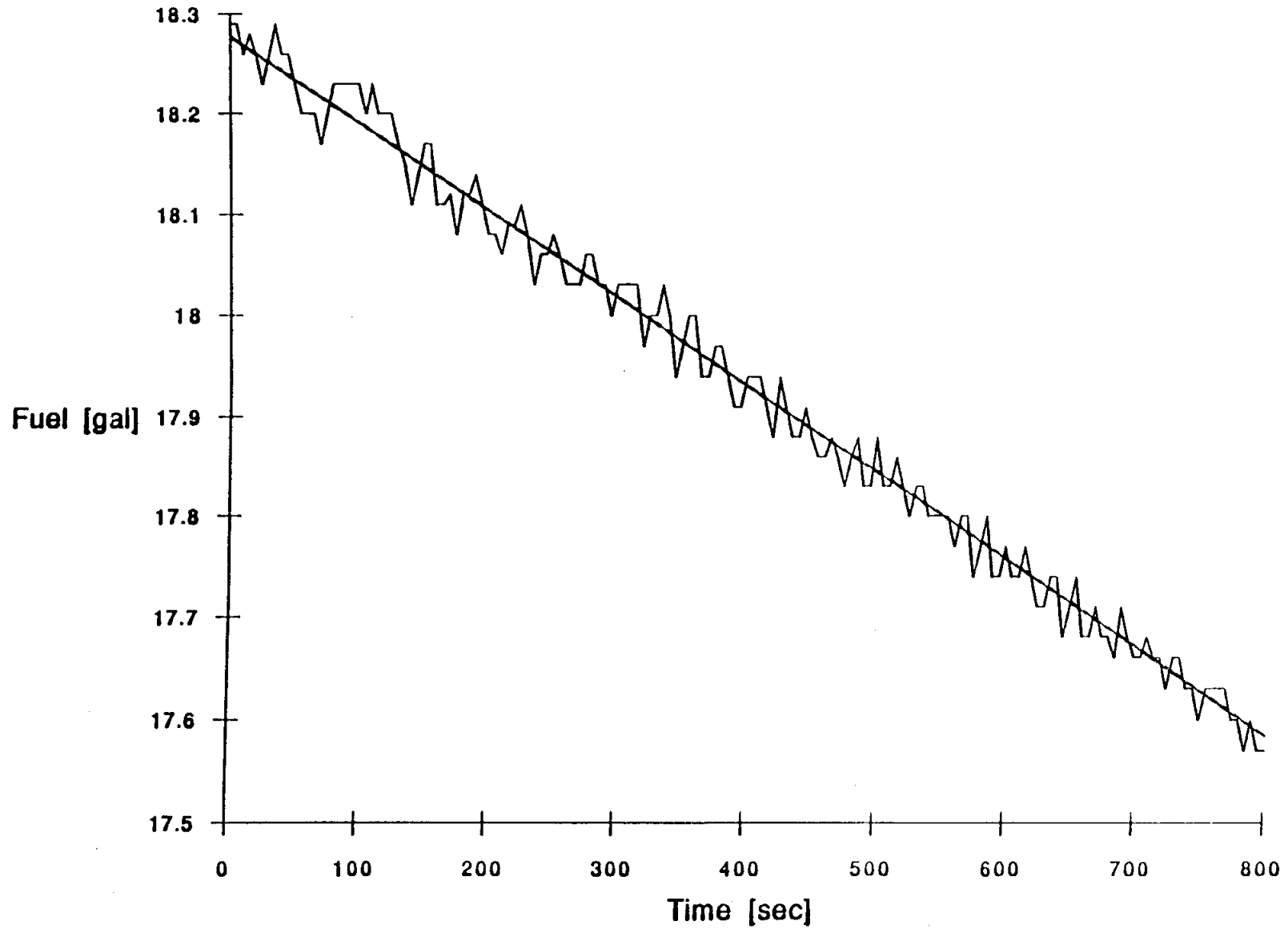


Figure 16. Fuel usage for 40 kW unmodified run using 45 kW generator set

vibrations in the diesel system. By taking an average slope over many minutes, we can reduce the influence of these fluctuations on our calculated fuel consumption rate to acceptable levels. The shop water heat rate, or heat flow, (Figure 17) is seen to reach a steady state value after 30 minutes or so.

Sample calculations for the 10 kW restricted flow final run appear in Appendix I for the steady state portion. The specific heats of the shop water and jacket water were taken to be that of water and the glycol-water mixture respectively. For the efficiency calculation, the higher heating value of number one diesel oil (19,240 Btu/lbm) (Taylor, 1985) was used. At a density of 54.6 lbm/ft³, this corresponds to 140.4 K Btu/gal.

Discussion of Results

One often cited rule of thumb for assessing the cogeneration potential of diesel-electric systems is that about 30% of the energy in the fuel appears ultimately as electric power, 30% as jacket water heat, and the same as heat energy flowing up the exhaust stack (cf. Figure 18). The remaining 10% is converted into radiative and other losses from the engine and generator envelopes. Information supplied by KEM Equipment (Appendix A) for full load conditions reveals a slightly better performance than provided by this generalization. In particular, at full load corresponding to a mechanical output by the engine of 50 kW, the fuel usage is given as 12.9 l/hr for number 2 diesel fuel, which translates to an energy input at a rate of about 138 kW. The quoted heat rejection rates under this condition to both the coolant and

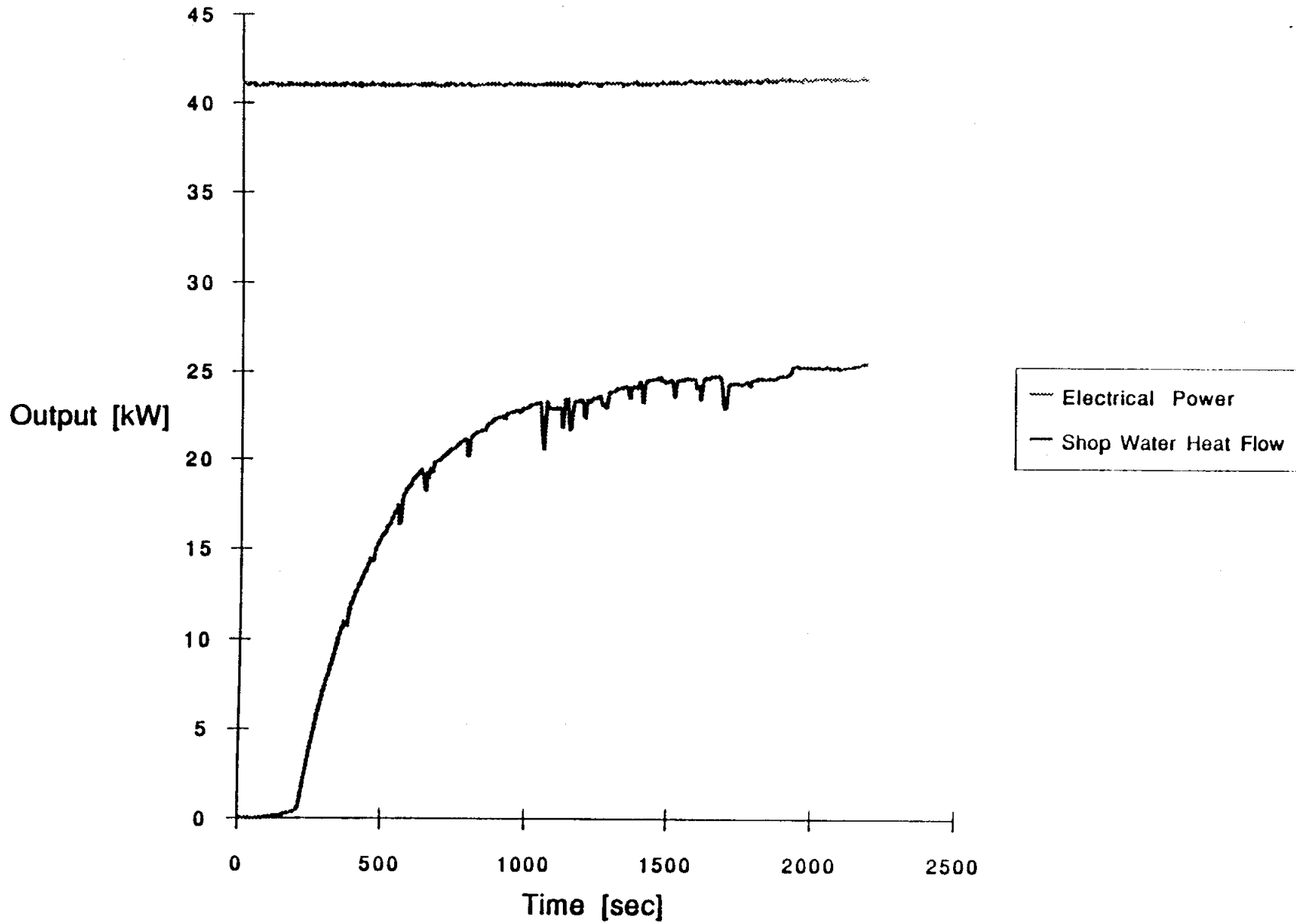


Figure 17. Thermal and electrical outputs for 40 kW unmodified run versus time using 45 kW generator set

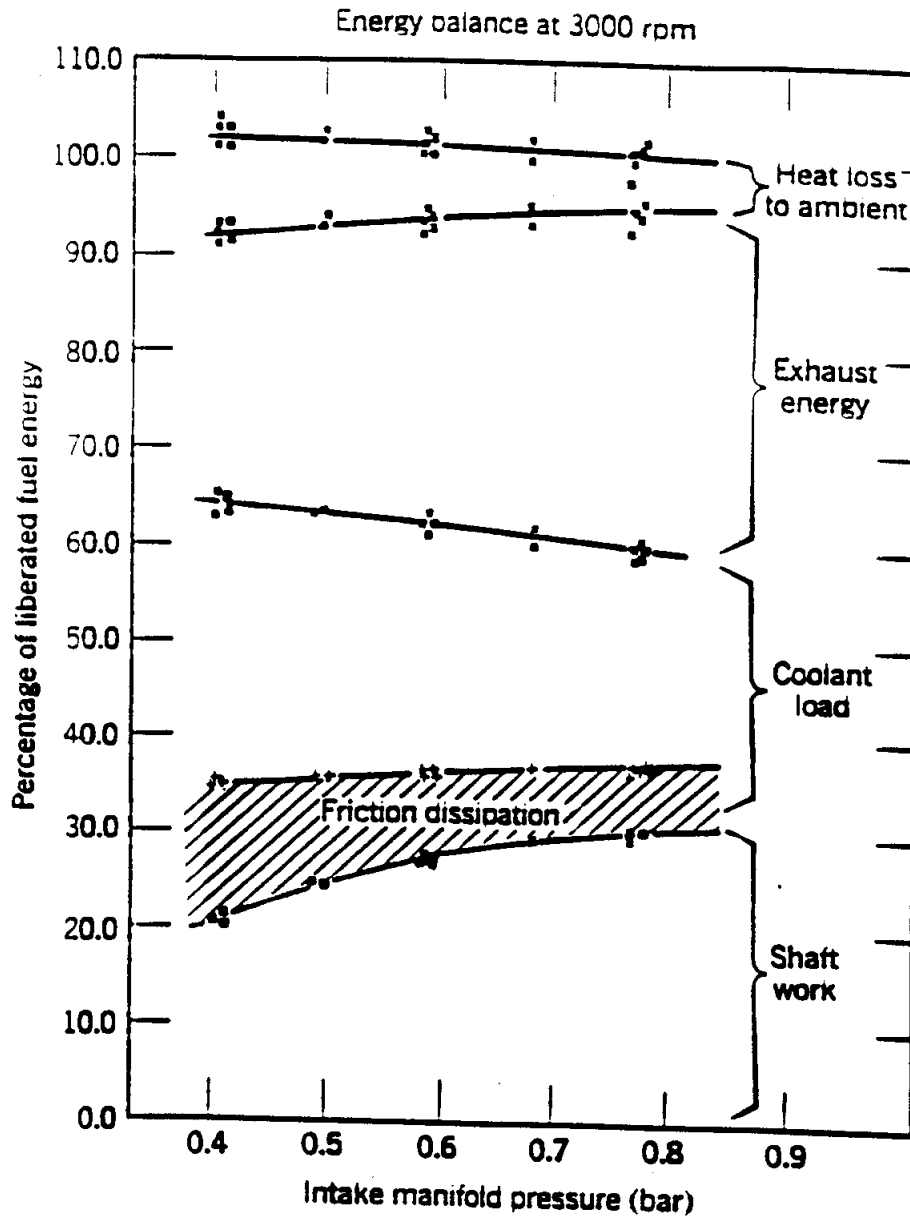


Figure 18. Energy balance for generator set (from Ferguson, 1986) (Actual data are for internal combustion engine.)

exhaust is around 31 kW. The heat radiated to ambient is given as around 6 kW. Hence, the first two heat rejection rates are each about 22% of the input energy rate and the mechanical power output is about 36% of the input. If we assume a generator efficiency of 90%, the electric power output is about 32% of the input. Our maximum electrical power output is about 45 kW for our particular engine generator pair.

At our maximum load tested in the normal operating mode, 41.7 kW, we measured an electrical efficiency of 32.1% and a 32.0 kW heat rejection rate to the jacket water (Table 2b). This efficiency is close to what we would infer from the manufacturer's specifications. We did not measure exhaust gas flow rate and hence could not calculate heat rejected to the exhaust gas from our data. If we assume the same rate of heat radiated to the ambient, 6 kW, and utilize our measured input energy in the fuel of 130 kW, then the heat rejection rate up the stack would be about 44 kW. We have incorporated a generator efficiency of about 90%. Here, based on Figure 16, we are simply satisfying conservation of energy,

$$\dot{Q}_h = \dot{W}_{el} + \dot{Q}_{jw} + \dot{Q}_{ex} + \dot{Q}_{rad} + \dot{W}_f \quad (4)$$

where, \dot{Q}_{jw} and \dot{Q}_{ex} are the rates of heat rejection to the jacket water and exhaust respectively, and \dot{Q}_{rad} represents the miscellaneous heat losses from the engine. The last term \dot{W}_f represents the losses involved in converting the mechanical output from the engine into electric power. This leads to heat dissipation from the generator to the surroundings and is about 6 kW under the above conditions according to manufacturer's

specifications. Hence, to achieve an electrical output of 41 kW, the mechanical output from the engine should be around 47 kW.

To provide an independent estimate of the exhaust gas heat rate, we will first use the manufacturer's value of 124 cfm for inlet air at full load (50 kW output from the engine) and our measured inlet and stack temperatures of 100 and 978°F respectively from Table 1b. This allows us to calculate a heat loss rate of about 34 kW from

$$\dot{Q}_{ex} = \dot{m}_c c_p (T_{ex} - T_{in}) \quad (5)$$

where \dot{m}_c is the mass flow rate of the products of combustion up the stack, c_p is the specific heat of the combustion products, T_{ex} is the exhaust gas temperature entering the stack, and T_{in} is the inlet air temperature. Here, we assume the properties of the exhaust gas are those of air with $c_p = 0.24$ Btu/lbm/°F and have assumed the inlet air density is 0.073 lbm/ft³. This calculation is lower than our prior estimate of exhaust heat rate calculated from an overall energy balance on the entire system by about 20%. This is not surprising as we are estimating several quantities such as exhaust mass flux and heat radiated. Moreover, to be conservative in our efficiency calculations, we utilized the higher heating value of the number 1 diesel fuel. If, instead, we had used the lower heating value of 133.2K Btu/gal (Taylor (1985)), \dot{Q}_h would have been 123 kW and $\dot{Q}_{ex} = 36$ kW from Eqn. (4), which is very close to that predicted from Eqn. (5). This lower heating value, which assumes no water vapor condenses after combustion, is compatible with a stack temperature of 978°F.

From Tables 2a and 2b or Figure 9, one can see that the heat rejection rate to the shop water versus electric load has a slope slightly less than one, meaning an increasingly higher percentage of the output energy shows up in the shop or jacket water as the load decreases. This is consistent with the efficiency results appearing in Figure 11. This figure reveals that the total system efficiency can remain relatively flat with load if cogeneration is utilized because the decrease in the electrical component is almost compensated for by an increase in the thermal component. Although we have not directly measured the exhaust heat rate, we can assume that it can be estimated from Equation (4) and the data in Tables 2a and 2b, assuming that the last two terms are relatively insensitive with load. For example, for the 11.1 kW normal run on Table 2b, assuming the last two loss terms in Equation (4) still add up to about 12 kW, \dot{Q}_{ex} must be about 6 kW. This probably represents a lower bound as extraneous heat losses from the engine and generator are less at the lower loads than at full load. For this run, the measured electrical efficiency is 26.0%.

It should be mentioned that this efficiency is 2% to 3% higher than those for the other runs conducted at the same load (Tables 2a and 2b). We believe the reason for the higher efficiency corresponding to a lower fuel consumption is a higher engine operating temperature for this particular test than for the initial normal run. This, in turn, was caused by both a lower shop water flow rate and the fact that this run was preceded by several hours of runs at higher loads. The other two nominal 10 kW normal final runs appearing on Tables 1b and 2b were conducted after a twenty minute warm-up at 40 kW. These two sets of

data are consistent with the idea that lower shop water flow rates (and hence less cooling capacity) at low power levels help increase efficiency. The other 10 kW runs were not immediately preceded by tests conducted near full load conditions. Hence, this particular test could have resulted in smaller frictional losses due to better lubrication at more desirable operating temperatures. We should also mention that for both the normal and restricted runs, the electrical efficiency did decrease as the shop water flow rate increased above one gpm and hence the oil temperatures decreased.

The electrical efficiencies for the restricted cooling runs don't appear to be different in a statistically significant way from the normal runs (Tables 2a, 2b and Figure 10). It should be noted that the reason the former were performed was primarily to see if higher engine temperatures could be maintained at low loads than for the normal mode of operation. In this sense, the experiment was a success in that the temperature of the jacket water leaving the engine was as much as 36°F higher for the restricted runs at the lower shop water flow rates than for the normal runs (Table 1a, 1b and Figure 5). In general, at a given load, jacket water outlet temperature increased as shop water flow rate decreased. Similarly, the oil temperatures were as much as 35°F higher for the restricted cooling runs (Figure 6). These elevated fluid temperatures at the low loads imply higher temperatures of the cylinder walls, which would presumably decrease the rate of carbon build up on the valves, rings, and cylinder walls at low loads. This, in turn, would prolong engine life. But, we didn't actually measure any of these latter temperatures.

The efficiencies for the heated intake air runs (Tables 2a and 2b) were higher than for the other runs at the lowest power levels if we ignored the 9 kW power input for the air heater. However, if this were included in the denominator of Equations (2 and 3), the electrical and cogeneration efficiencies fell below those of the other two operational modes at all power levels. This is because not all the energy in the inlet heated air stream is able to be converted into useful heat and power, plus the hotter inlet air is less dense than the ambient so the mass flow of inlet air is reduced.

A critical component of this work is our ability to measure temperatures, flow rates, and electrical power accurately. For type T thermocouples used to measure liquid temperatures, the error limits around 200°F were around $\pm 0.7^\circ\text{F}$. For the type K around 750°F, the error limit is about $\pm 3^\circ\text{F}$. We typically used temperature differences between inlet and outlet of a particular component to calculate energy gains and losses. For the shop water and stack gases, this difference was at least 30°F so the error of a given thermocouple was no more than about 2% of the difference. In fact, the uncertainty in the temperature difference for the type T thermocouples is given by

$$\xi(T) = [(0.7)^2 + (0.7)^2]^{0.5} = 1.0^\circ\text{F} \quad (6)$$

But, with both thermocouples coming from the same roll, this result would be highly unlikely (Holman, 1989). Hence, we expect an error of less than 1.0% for these temperature differences. The key temperature difference measurement is that of the jacket water with the difference

being as low as 3.5°F and usually less than 10°F. This results in an error as high as 28% for an uncertainty in temperature difference of 1.0°F. But, independent calibration tests reveal the bare thermocouple junctions produce results within about 0.3°F of each other when measuring the same temperature. This results in a temperature uncertainty of about 0.4°F, which leads to a maximum error of 11% with a characteristic error for the data shown being normally under 10%.

Another effect that is important in analyzing the data is the difference in temperature between a bare thermocouple junction immersed in the flow and a thermocouple junction inserted in a well. Independent tests we conducted indicate the latter tended to produce temperatures from about 1°F to 4°F lower than the former at temperatures between 120°F and 212°F. This information is needed to evaluate the error in the jacket water heat transfer rate for the initial runs, since the thermocouple used to measure the jacket water temperature after the heat exchanger prior to returning to the engine was immersed in a well, while that used to measure the temperature of the jacket water leaving the engine was a bare junction immersed within the flow but adjacent to the wall. Hence, the actual change in temperature for the jacket water could have been as much as 4°F lower than what one would infer from Tables 1a and 1b.

These findings led us to look for a better way of measuring jacket water inlet temperature for the final set of runs. We found the best solution was to fill the wells with a highly conducting gel, Dow Corning 4 compound. It maintains a grease-like consistency over a wide temperature range. We carefully tamped it into the wells, taking care

not to form an air pocket, and performed a series of experiments. We found that, in the temperature range of interest for the jacket and shop waters, a thermocouple in the gel-filled well read within 0.2°F of a bare thermocouple bead inserted in the same warm liquid. This was much better than even a well filled with a silicon gasket material. Since our desire was to measure jacket water temperature differences to within 1°F, we repeated many of the initial runs using these wells. At the same time, we also collected additional data at different shop water flow rates. This resulted in the data on Table 1b.

The 0.5" and 2.0" turbine flowmeters are rated by the manufacturer as having an accuracy of $\pm 0.5\%$ of the reading, with the smaller meter rated from 1.25 to 9.5 gpm and the larger from 15 to 225 gpm. The data on Tables 1a and 1b indicate we were almost always within this range. Our independent calibration verified that these meters were reading the actual flows to within about 2%. We did not attempt to incorporate enough accuracy into our analysis to verify the 0.5% figure. We found that the 2" meter didn't measure flows less than about 5 gpm and tended to read too low for flows less than 10 gpm.

These ideas can now be utilized in evaluating our energy balance calculations for the heat exchanger. The results on Table 2a indicate the heat gain by the shop water is from 18% to 40% less than the heat lost by the jacket water. Much of this difference is due to the jacket water temperature difference being possibly more than 1°F too high because only the low temperature thermocouple lead was embedded in a well. If we just decrease all the values for \dot{Q}_{jw} correspondingly, the

two values are closer together, with the biggest difference being 28% and half of the pairs being within 15% of one another. Other calculations (Appendix I) indicate a maximum rate of heat transfer from the heat exchanger plus the nine foot hose to the surroundings due to radiation and convection of 0.7 kW. Adding this correction to a first law analysis for the heat exchanger results in energy being conserved to within 20% in all cases except for the 40 kW data for the initial runs. For half of the runs, a 1°F correction in the jacket water inlet temperature is enough to satisfy conservation of energy for the heat exchanger. For the other runs, a correction of up to 3°F is required. This is certainly plausible in light of our accompanying experiments with thermocouple accuracy.

In any event, the data on Table 2b indicate that the heat loss by the jacket water is invariably within 6% of the heat gain by the shop water when the temperature difference for the jacket water is measured more accurately.

We should mention that these tests were not designed to test the performance of an optimally-sized heat exchanger to recover jacket water heat. One purpose was rather to show that the potential exists for improved system performance due to jacket water heat recovery even at low loads. The data on Table 2 certainly indicate this to be the case. The heat exchanger that was evaluated was simply supplied by the vendor as a means of cooling the engine. It was large enough to cool the jacket water by a few degrees Fahrenheit and consisted of an 8" diameter shell filled with one inch diameter tubes. It was not insulated, but a

heat exchanger in a cogeneration application should be insulated to allow a greater percentage of the jacket water heat loss to be transferred to the cool side of the heat exchanger.

PERFORMANCE OF 80 KW GENERATOR

Apparatus

The second location at which our data acquisition system was deployed is the DOT&PF maintenance camp at Coldfoot as mentioned earlier. This facility has a generator building with three generator sets of which only two are operational. The two operational units of 80 and 100 kW capacities are cycled so that each unit operates for 10 days at a time. The unit whose performance we evaluated is a Caterpillar 3304B generator set with a rating of 80 kW prime operating at 1800 RPM. As detailed in Appendix J, this unit consists of a four-stroke turbocharged watercooled diesel mated to a CAT SR4 generator. The latter produces three phase electric power at 480 volts.

The electric power produced is used for lighting and various electrical machinery such as pumps and fans, while some of the jacket water heat is captured by an externally mounted heat exchanger to provide heat for a garage. There is also an externally mounted radiator to provide cooling capacity in case the demand for waste heat is not sufficient to provide adequate cooling. In this project, we are particularly concerned with the rate at which heat is supplied across the heat exchanger. As shown in Figure 3, the ethylene glycol coolant is used to transfer heat from the engine to either the radiator or the heat exchanger flows through 2

inch diameter lines. The apportionment of this flow between the radiator and heat exchanger is controlled by an Amot valve. When there is a high demand for heat, the majority of the flow is diverted toward the heat exchanger. Of course, if the engine temperature is not sufficiently high, the block mounted thermostat will not fully open and most of the flow will simply recirculate within the engine until the operating temperature reaches about 178°F. Then, the thermostat will open fully with the high temperature shut off at 192°F.

The heat exchanger is a Bell and Gossett GPX 130 Plate Heat Exchanger. As detailed in Appendix K, it has a maximum flow rating of 245 gpm and consists of 15 plates having a surface area of about 1.3 ft² per plate. The flow is counterflow with hot and cold fluid alternating between plates. We measured flows on either the hot or cold sides as no more than about 20 gpm.

The sensors we installed consisted of a power transducer, thermocouples, and flowmeters. The transducer is an Ohio Semitronics 150 kW, 480 V, 3 phase, 4 wire unit with a delta connection and 10 V full scale output (Unit 74B in Appendix D). The thermocouples are type J and the flowmeters 2-inch turbine meters with pulsed output (Appendix L). The signals from these were fed into the same model (Campbell 21X) datalogger used for the 45 kW unit. All the data were collected every 15 minutes during the ten days the 80 kW unit operated. Because of system problems, we did not always collect 10 days worth of data each time the unit operated. We collected data for a total of 24 days from mid-January until mid-May, 1989. The data were incomplete for the first

12 days because the data logger experienced some overflows in several of the final storage locations. This was corrected for the next set of data collection. Other system problems included shut downs due to (1) air in the coolant lines leading to excessive vibration and (2) problems with the temperature regulating unit on the diesel engine.

By measuring both the flow into the radiator and into the heat exchanger on the hot side, and the temperature of the fluid leaving the radiator, we can calculate how much of the heat being rejected to the jacket water is ultimately leaving the system via the radiator and how much via the heat exchanger using Equation (1). The rate of heat gain by the propylene glycol on the cold side of the heat exchanger represents the rate of heat being delivered to the garage.

Results

We tried to utilize an existing totalizing flow meter to measure the fuel consumption of the generator set. However, the return flow from the engine was fed back into a day tank instead of downstream of the totalizer. Hence, the totalizer readings overestimated the diesel fuel usage (no. 1 heating oil). However, since the kW output of each generator set used normally stayed within a relatively narrow range (from about 45 to 55 kW) and data were available for the totalizer reading every day, we were able to approximate the daily fuel usage. We did this by taking the minimum daily totalizer reading which was 90 gallons on Julian day 70. Since the totalizer provides an upper bound on generator fuel usage, the minimum of all the daily values should be close to the actual fuel usage. This amount of 3.75 gph at an average

load of 50 kW corresponds to an efficiency of 32%. This is consistent with manufacturer's specifications as provided in Appendix J.

The average values of the raw data for 12 days of testing from February 15, 1989 until May 30, 1989 appear in Table 3. The reduced data on Table 4 shows the heat delivered to the radiator, and to and from the heat exchanger. On Figure 19 is a plot of heat delivered as a function of ambient temperature. It is seen that there is no obvious correlation with temperature. Limited data (not appearing on Table 3) were collected for 12 days from January 23 through February 3, 1989. During this period, the outdoor air temperature was extremely low, the daily mean temperature for the January portion being -50°F or colder. The heat delivered to the cold side of the heat exchanger varied between 12.5 and 17.8 kW while \dot{Q}_{hs} varied between 16.3 and 20.8 kW. The electric power output varied between 49 and 61 kW. The jacket and shop water temperatures also were comparable to those appearing in Table 3.

In considering the heat delivery rate, one should keep in mind that the primary source of heat for the 5,000 ft² shop is a 130 K Btu/hr oil furnace. This runs much of the time during the winter, hence supplying heat at a rate of over 30 kW, since 130 K Btu/hr is equivalent to 38 kW. The set point for the heat supplied by the jacket water is 5°F above that for the furnace (Drygas, 1989).

Discussion of Results

The results appearing on Figure 19 and Tables 3 and 4 represent daily averages of various energy parameters. Some of these averages are very

Table 3. Coldfoot data. Average daily temperatures and flows

Day Julian Time	Average Temperature ($^{\circ}\text{F}$)			
	T_{jh}	T_{jc}	T_{sc}	T_{sh}
46	172.9	151.1	117.9	122.6
47	173.8	152.9	117.6	122.5
48	174.3	152.8	116.7	122.4
49	177.7	160.3	117.2	124.7
66	170.0	143.2	117.9	122.0
67	171.0	144.6	118.0	122.0
68	171.8	144.0	118.5	122.3
69	171.7	142.7	118.0	121.7
70	171.7	143.1	117.7	121.6
71	172.1	143.5	117.6	121.6
72	171.7	142.9	117.6	121.4
73	171.9	143.4	117.4	121.3

Day Julian Time	Average Temperature ($^{\circ}\text{F}$) and Flows (gpm)				
	T_a	T_r	\dot{V}_{jw}	\dot{V}_{sw}	\dot{V}_{rad}
46	21.8	152.1	6.0	21.9	7.5
47	14.5	150.2	6.2	22.1	7.8
48	14.8	150.6	6.1	22.1	7.7
49	11.6	159.8	11.7	22.0	18.9
66	-9.5	118.1	3.9	22.8	4.1
67	-17.0	102.1	3.7	22.7	3.0
68	-13.5	107.5	3.7	22.8	2.9
69	4.8	104.4	3.9	22.0	3.8
70	7.8	92.5	3.8	21.9	3.5
71	14.2	105.7	4.0	21.8	3.6
72	13.9	101.8	3.9	21.8	3.3
73	4.3	100.0	4.2	22.0	3.9

Notes: T_{ex} measured on day 73 at 697°F .

Table 4. Coldfoot data. Average daily heat flows and electric power

Day Julian	\dot{Q}_{hs}	\dot{Q}_{rad}	\dot{Q}_{cs}	\dot{W}_{el} Power	$\dot{Q}_{cs}/\dot{Q}_{hs}$	$\dot{Q}_{hs} + \dot{Q}_{rad}$
46	15.9	15.8	13.5	46.4	0.86	31.6
47	15.7	18.2	14.2	46.9	0.94	33.8
48	15.8	17.2	16.6	44.4	1.13	33.0
49	20.6	17.9	21.8	47.4	1.16	38.5
66	12.9	18.0	12.2	56.6	0.99	30.9
67	12.5	14.6	11.7	53.1	0.98	27.1
68	12.8	13.5	11.8	51.9	0.92	13.5
69	13.9	14.6	11.7	47.1	0.89	28.6
70	13.6	13.3	12.1	46.8	0.92	26.9
71	14.2	14.5	11.8	47.4	0.87	28.7
72	13.8	11.6	11.9	45.9	0.90	25.5
73	14.9	15.8	11.9	46.7	0.80	30.7

Note: "el" is the electric power output, "hs" refers to the hot side of the heat exchanger, and "cs" refers to the cold side.

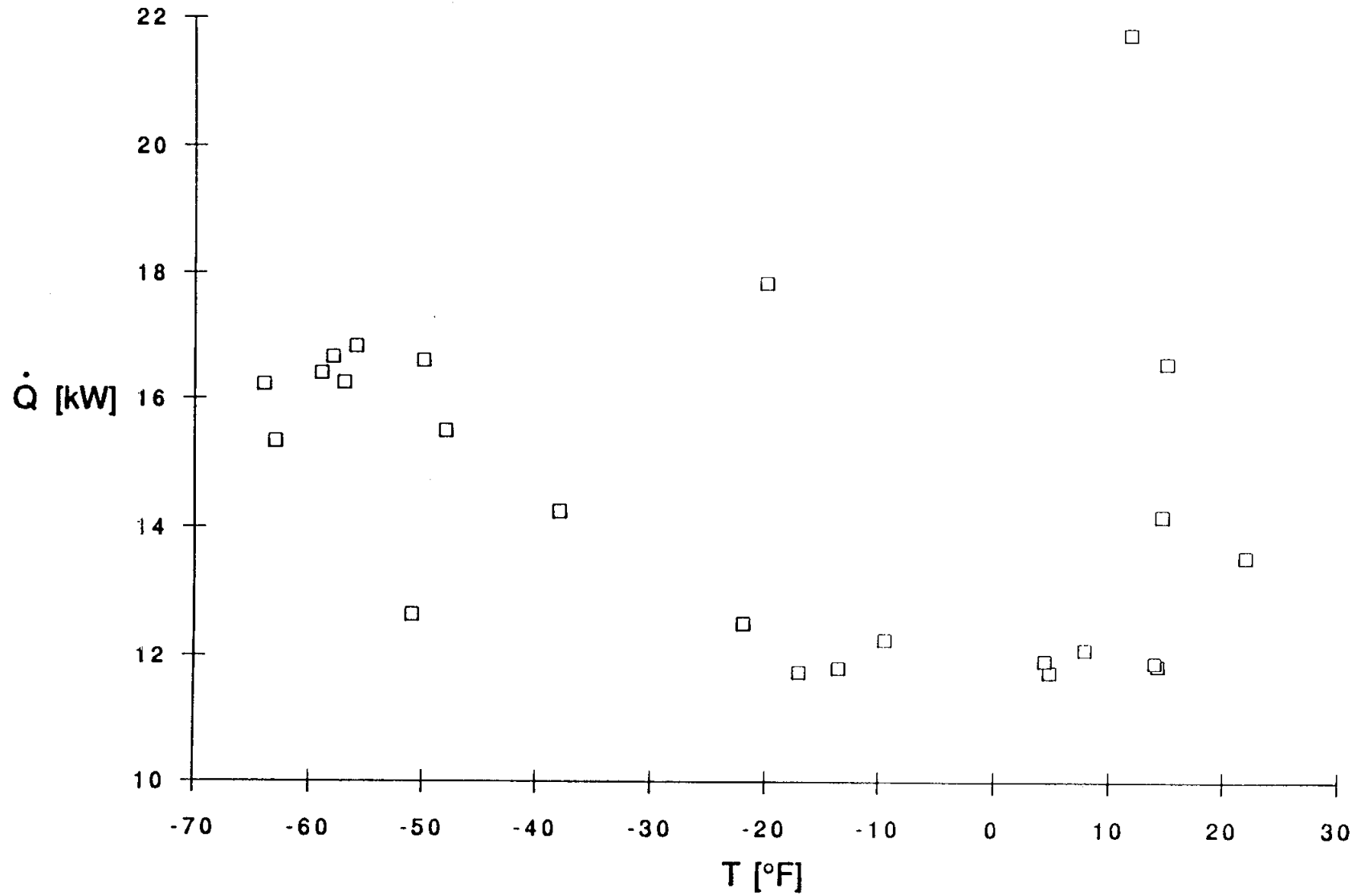


Figure 19. Heat delivered versus outdoor air temperature for 80 kW generator set

close to the 15-minute values also, some of which are shown in Appendix N. For example, the 15-minute electric power values vary from 35 to 70 kW, but over 90% of the values were within 20% of the average daily values. The liquid flow rate on the cool side of the heat exchanger only varied from 21.4 to 23.4 gpm in terms of 15-minute values. The former is consistent with the electric loads while the latter is consistent with the 1/2 HP centrifugal pump operating in a fixed piping network.

From Table 4, one can see that the daily heat gain by the propylene glycol on the cool side of the heat exchanger averages about 95% of the heat loss from the ethylene glycol on the hot side. The difference is due to the losses through the heat exchanger shell, since it was not insulated, plus uncertainties due to our inability to measure temperatures and flow rates with 100% accuracy. These will be discussed shortly. In any event, the heat delivery rate to the garage is significant, around 13 to 20 kW in January and February, 1989, and around 10 kW in March. This should be compared with the baseline heat source which is a 130K Btu/hr oil fired boiler (38 kW). Hence, cogeneration is supplying one-fourth to one-half as much heat as the primary heat source if the latter were performing at its maximum capacity.

The thermocouples used to measure liquid temperatures were commercial grade type J with limits of error of $\pm 4.0^{\circ}\text{F}$ or .75%. Via Equation (6), this would produce an error of $\pm 5.2^{\circ}\text{F}$. This could produce a very significant uncertainty in trying to measure the temperature difference

on the cold side of the heat exchanger. From Table 3, this difference is of the order of 5°F. However, since all the thermocouple probes were constructed from the same roll of thermocouple wire, one would expect the uncertainty to be much less. We performed our own calibration by immersing the junctions in a heated ethylene glycol-water bath (50/50) and letting the temperature vary from 75°F to 219°F. We found that four different thermocouples were almost always within $\pm 0.2^\circ\text{F}$ of each other and checked to the same accuracy with a precision mercury in glass thermometer. Using this uncertainty produces an error of about $\pm 0.3^\circ\text{F}$ in measuring a temperature difference. Hence, we would expect the error in \dot{Q}_{CS} due to temperature uncertainty to be less than about 6%. On the hot side, the average temperature difference is more like 20°F to 30°F, so we expect less than a 2% uncertainty in \dot{Q}_{HS} due to temperature.

We believe our shop water flow rate is known to within 1% since we are within the recommended flow range for the 2-inch turbine flow meters. Unfortunately, for almost all the data (the exception being day 66), there are substantial uncertainties in jacket water flow rates both to the primary side of the heat exchanger and to the radiator. The indicated average daily flows during these days were less than 8 gpm with one less than 1 gpm if we use all the 15 minute data. The recommended range for these 2-inch meters is from 15 to 225 gpm. Our own calibration indicated these meters tended to read from about 10% to 30% too low in the 8 gpm actual flow range and were more than 100% too low for flows less than 6 gpm. This is the most likely explanation as to why \dot{Q}_{HS} was less than \dot{Q}_{CS} for much of the data on Table 4.

To concentrate on those data points which have the greatest validity, we have disregarded all the 15-minute data points for which any indicated fluid flow rate was zero in computing flows and heat transfer rates. This occurred frequently on days 66 through 73 but not at all on days 46-49. The ratio of heat transferred to the cold side to that transferred from the hot side of the heat exchanger varied from 80% to 116% in terms of average daily values. Here the average daily values are averages of the 15-minute ratios. The 15-minute values for this ratio varied even more. The main reason for the values being significantly different from 1 is the inability of the flow meters to monitor flows less than 5 gpm. On many days, the majority of the 15-minute indicated flows to the hot side of the heat exchanger were less than 5 gpm. Another reason for the measured heat rate into the heat exchanger being larger than \dot{Q}_{CS} is due to the fact that the heat exchanger is not insulated. Assuming an average surface temperature of around 140°F and a surface area of about 22 ft² allows us to calculate a gross radiation heat loss rate of the order of 1 kW. Here we have used the Stefan Boltzman Equation for a black body and have neglected reradiation back to the heat exchanger (Lienhard, 1987). This is from 5% to 10% of the heat gain rate by the glycol-water mixture going to the shop. Similarly, the rate of heat loss from the 30-foot-long copper pipe between the engine and heat exchanger should be less than 0.5 kW. The temperature of the jacket water entering the heat exchanger is measured about 4 ft. upstream from the exchanger and about 15 ft. downstream from the engine (Figure 3).

It should be mentioned that we used 2-inch meters because (a) the lines were 2 inch and (b) the jacket water flow is rated at 40 gpm (Appendix J). Moreover, the heat exchanger was rated at 225 gpm maximum (Appendix K). The engine has a thermostat that opens fully at 178°F and shuts the system down at 192°F (Bishop, 1989). Hence, one would expect most of the jacket water flow to bypass the external cooling system and be recirculated within the engine until its temperature exceeded 178°F. From looking at the data on Table 3, one can see that the average daily jacket water temperature leaving the engine only approached 178°F on one day (49) and was always less than or equal to 172°F on every day after that. Hence, there was little jacket water leaving the engine in March leading to spurious data for the flows to the hot side of the heat exchanger and the radiator. But, from the fact that heat was transferred to the cool side of the heat exchanger at a rate of around 10 kW during this period, there must have been some jacket water flow. If one uses the measured jacket water temperature drop across the heat exchanger together with the heat transfer rate of 10 kW, one concludes that the jacket water flow rate to the hot side of the heat exchanger must have been around 2 to 3 gpm, too low to be recorded by our flow meters. These low flows, which correspond to low jacket water temperatures, occurred after the B200 temperature control unit was replaced.

ECONOMIC CONSIDERATIONS

Clearly, there are incentives for operating equipment as efficiently as possible and providing heat and power to buildings and communities as cheaply as possible. In cold climates during the heating season, the

heating needs are often much greater than the electrical needs in terms of rate of energy consumption. Hence, there is a real incentive to recover heat by employing cogeneration as part of the electrical generation process. We have shown that even at low loads, there is a supply of available heat in the jacket water that could be utilized to provide space heating needs. In measurements taken over a three month period in early 1989, we found that heat recovery at the rate of 10 to 20 kW was occurring at the DOT&PF maintenance camp in Coldfoot, Alaska from an 80 kW generator set. Although the 5,000 ft² garage that was heated with this energy had much of its heating needs supplied by a 130K Btu/hr boiler, this recovered heat was significant.

In fact, if we perform a simple economic analysis, we can calculate a payback period of five to six years for the installation of heat recovery from the jacket water. Let us start with the existing diesel electric generator in the generator building plus the boiler in the garage. To their baseline costs, we must add the cost of the heat exchanger plus the associated piping and controls. The former is \$1757 FOB Seattle (Larry Harrington, 1989). Other items are: two 50K Btu/hr unit heaters in the garage at \$700 each, an expansion tank at \$50, two one-half hp pumps at \$150 each, and several control valves costing around \$1,500. The price of the several hundred feet of 2" and 1" copper lines with elbows needed to transport the propylene glycol water mixture to and from the unit heaters and heat exchanger is around \$1,600 (Swagger, 1989). Hence, we will estimate a capital cost of roughly \$6,500 plus \$2,000 for shipping. We will approximate the installed cost

of the heat recovery system as double the capital cost FOB Coldfoot. This results in an estimate of \$17,000.

Assuming an average heat delivery rate of 15 kW over a 10 month prime heating season, a total of about 368 M Btu of heat would be delivered to the garage. At a net heat delivered around 100 K Btu/gal of heating oil, this is equivalent to 3,680 gallons of heating oil saved per year. At a cost of about \$1.00/gal (Drygas, 1989), this translates to a savings of fuel oil equivalent to about \$3,700 annually. Hence, the simple payback period is under five years. From another perspective, the yearly amortization on \$17,000 at an annual rate of 10% over 10 years is \$2,800. Hence, the yearly savings (assuming no upkeep is required on the heat recovery system) is about \$900. If we used 8% over 15 years, the yearly savings increase to \$1,700.

This positive result follows, even without capturing waste heat from the exhaust. There is approximately as much heat there to be recovered as from the jacket water. Capturing a good portion of this could double the savings in fuel oil costs by reducing the amount of heat required from the furnace. Of course, if this strategy were pursued, one would have to be especially careful with stack corrosion due to the formation of sulfuric acid in the exhaust and accompanying condensation if the stack temperature falls below the dew point. It also follows even without considering the extra lifetime of the shop furnace resulting from its needing to operate fewer hours per year. These furnaces may only last five years normally (Drygas, 1989). We could also use electrical resistance heating to capture still more heat if the

generator set capacity is underutilized. Use of the latter as load banks would be prudent if the degree of part-loading is extreme (under 20% of capacity, say, (Malosh et al., 1988)).

CONCLUSIONS

- (1) The total part load efficiency of diesel-electric generators can be considerably enhanced if heat is recovered from the jacket water as electricity is produced. In particular, we found a total efficiency of over 50% for loads greater than 10 kW for a 45 kW generator set.
- (2) Engine operating temperatures and presumably system lifetimes can be enhanced at part loads by restricting the cooling available for the jacket water at low loads. At loads between 10 and 20 kW on a 45 kW generator set, we were able to increase oil and jacket water outlet temperatures by over 20°F.
- (3) Appreciable amounts of heat are available in the hot jacket waters of systems now operating throughout rural Alaska. Data we collected at the DOT&PF camp at Coldfoot indicate that heat is being recovered at a rate in excess of 10 kW. This is equivalent to an annual fuel savings in excess of \$3,600.
- (4) System performances including heat recovery can be monitored using standard hardware for measuring flow, temperatures, and electric power. However, one must be careful in evaluating heat transfer across heat exchangers to accurately measure temperature changes

of the hot and/or cold fluids when such changes are small. We found that filling thermocouple wells with a highly conducting gel was very helpful in this regard.

- (5) A data acquisition package can be obtained for around \$5K to measure the appropriate physical parameters. This does not include the cost of a personal computer nor software needed to manipulate the data. Any one of several spreadsheets available for several hundred dollars can be used for the latter.

REFERENCES

Alaska's Energy Plan. 1986. Department of Commerce and Economic Development and Alaska Power Authority, Anchorage.

"Load Banks for Diesel-Engine Generator Applications." n.d. Reprinted from Diesel and Gas Turbine Progress. Avtron Manufacturing, Inc., 10409 Meech Ave., Cleveland, OH.

Bishop, R. 1989. N.C. Machinery, Seattle, WA. Personal communication.

Campbell, A.S. 1979. Thermodynamic Analysis of Combustion Engines. John Wiley & Sons, New York.

Cerigo, P., and R. Ronton. 1984. Energy demand and cost in Canadian remote communities. Atomic Energy of Canada Ltd., Ottawa, Ontario, Rpt. R10A-1.

- Doolittle, J.S. 1964. Thermodynamics for Engineers, 2nd edition. International Textbook Co., Scranton, PA.
- Drygas, M. 1989. Alaska DOT&PF Maintenance and Operations, Fairbanks, AK. Personal communication.
- Ferguson, C. 1986. Internal combustion engines. John Wiley & Sons, New York. 540 pp.
- Frost and Sullivan. 1985. The worldwide market for remote power systems, Vol. II. Frost and Sullivan, Inc., New York.
- Hansen, P. 1987. Alaska Power Authority, Anchorage. Personal communication.
- Larry Harrington, Inc. 1989. Portland, Oregon. Personal communication.
- Holman, J. 1989. Experimental methods for engineers. McGraw-Hill, Inc. New York.
- Johnson, R., C. Hok and M. Bauer. 1987. Economics and Reliability of Diesel Electric Generators. Phase 1. Final report submitted to Alaska Department of Transportation and Public Facilities. Fairbanks.

- Keiser, G. and O.A. Hoke. 1985. Rural energy: An overview of programs and policy. House Research Agency, Alaska State Legislature, Rpt. 85-C.
- Kirkwood, A.C. and Associates. 1981. Survey of diesel generation by small U.S. utilities. Prepared for Electric Power Research Institute, Palo Alto, CA. Report EPRI AP-2113.
- Lienhard, J. 1987. A Heat Transfer Textbook, Prentice-Hall, Inc., Englewood Cliffs, N.J.
- Malosh, J., R. Johnson and S. Bubendorf. 1986. Part load economy of diesel-electric generators, Alaska Department of Transportation and Public Facilities Rpt. AK-RD-86-01.
- Mulloney, J. 1986. Small-scale cogenerations technology. The Cogeneration Journal. 1:59-69.
- Raj Bhargava Associates. 1985. Rural Energy Construction Program 1984-1985. Alaska Power Authority, Anchorage.
- Sakhuja, R., and M. Koplw. 1986. Modular cogeneration systems. The Cogeneration Journal. 2:4-22.
- Swagger, W. 1989. Chandler Plumbing and Heating, Fairbanks, AK. Personal communication.

Taylor, C.F. 1985. The internal combustion engine in theory and practice. MIT Press, Cambridge, MA, Vol. 2.

Taylor, R., T. Londos, M. Khazra, and E. Williams. 1984. Alaskan remote site evaluation for fuel cell energy systems. Prepared for Belvoir Research Development and Engineering Center, Ft. Belvoir, VA. Rpt. DAAK70-84-D0053, T.O. No. 0005.

Implementation Statement

by DOT&PF Statewide Research Section

This report documents studies of cogeneration systems both in the UAF lab and at DOT&PF's maintenance camp at Coldfoot. The system at Coldfoot is typical of many used in remote locations in Alaska. Both systems showed that cogeneration can be practical and cost effective. Furthermore, cogeneration can produce savings of nonrenewable oil resources and reduce pollutant emissions.

The report will be distributed to DOT&PF staff responsible for remote site facilities.

Statewide Research is funding a demonstration project to retrofit heat recovery equipment at the Slana Maintenance Station. The system will be monitored and reported on at a future date. This project will bring further visibility to cogeneration systems and yield more information on their operation.

Waste heat recovery systems were recently installed on some of the equipment at the 7 Mile, Chandalar, and Sag River Maintenance Camps on the Dalton Highway. These were put together "on a shoestring" by Maintenance & Operations. Finding even small amounts of money in an operating budget for this sort of improvement is difficult.

The retrofit of heat recovery systems to existing generator sets needs further encouragement. Capital funding is warranted when long term cost savings can be demonstrated. It is important, however, that electronic controls and other components of remote systems be as reliable and simple as possible.

The modest capital requirements of retrofits might be accommodated by funding one or two annually. An alternative would be to establish a revolving fund sufficient to pay for two or three system conversions, with fuel savings returning to the fund in order to finance additional installations. This latter concept would require unusual financing and bookkeeping arrangements.

The implementation of this report's findings is simpler in cases where new or replacement generator sets are to be installed. It is Department policy to select capital improvements based on minimum life cycle costs. Cogeneration systems should be a considered alternative. The distribution of this report should aid in this process.

As discussed in the report, new diesel generator systems should be sized for immediate demands so that they will run near capacity, with additional units added if and when demand warrants them. For existing oversized systems which run at low loads, managers should consider retrofitting heating systems to maintain higher load factors and operating temperatures. As reported herein, load banks and controls to accomplish this are available and may reduce maintenance problems and expenditures.